



Research paper

A highly selective purine-based inhibitor of CSF1R potently inhibits osteoclast differentiation

Thomas Ihle Aarhus^{a,b}, Jan Eickhoff^b, Bert Klebl^b, Anke Unger^b, Joanna Boros^b, Axel Choidas^b, Mia-Lisa Zischinsky^b, Camilla Wolowczyk^{c,d}, Geir Bjørkøy^{c,d}, Eirik Sundby^e, Bård Helge Hoff^{a,*}

^a Department of Chemistry, Norwegian University of Science and Technology (NTNU), Høgskoleringen 5, NO-7491, Trondheim, Norway

^b Lead Discovery Center GmbH (LDC), Otto-Hahn-Strasse 15, 44227, Dortmund, Germany

^c Department of Biomedical Laboratory Science, Norwegian University of Science and Technology (NTNU), NO-7491, Trondheim, Norway

^d Centre of Molecular Inflammation Research, Department of Cancer Research and Molecular Medicine, Norwegian University of Science and Technology (NTNU), NO-7491, Trondheim, Norway

^e Department of Material Science, Norwegian University of Science and Technology (NTNU), NO-7491, Trondheim, Norway



ARTICLE INFO

Keywords:

CSF1R
PLX3397
Autoinhibited form
Purines
Osteoclast differentiation

ABSTRACT

The colony-stimulating factor 1 receptor (CSF1R) plays an important role in the regulation of many inflammatory processes, and overexpression of the kinase is implicated in several disease states. Identifying selective, small-molecule inhibitors of CSF1R may be a crucial step toward treating these disorders. Through modelling, synthesis, and a systematic structure-activity relationship study, we have identified a number of potent and highly selective purine-based inhibitors of CSF1R. The optimized 6,8-disubstituted antagonist, compound **9**, has enzymatic IC₅₀ of 0.2 nM, and displays a strong affinity toward the autoinhibited form of CSF1R, contrasting that of other previously reported inhibitors. As a result of its binding mode, the inhibitor shows excellent selectivity (Selectivity score: 0.06), evidenced by profiling towards a panel of 468 kinases. In cell-based assays, this inhibitor shows dose-dependent blockade of CSF1-mediated downstream signalling in murine bone marrow-derived macrophages (IC₅₀ = 106 nM) as well as disruption of osteoclast differentiation at nanomolar levels. *In vivo* experiments, however, indicate that improve metabolic stability is needed in order to further progress this compound class.

1. Introduction

The colony-stimulating factor 1 receptor (CSF1R) is a type III tyrosine kinase, which acts as cell-surface receptor for the cytokines colony stimulating factor 1 (CSF1) and interleukin 34 (IL-34). Upon cytokine binding, this kinase receptor promotes signalling, eventually triggering the release of proinflammatory chemokines and thereby regulates the survival, function, proliferation and differentiation of cells in the myeloid lineage such as monocytes, macrophages, microglia and osteoclasts [1]. Thus, targeting CSF1R may result in therapeutic effects in various diseases [2–4]. Among others, CSF1R signalling is of importance in bone remodelling, a process which is regulated by different bone cells. The osteoblasts are responsible for bone build-up, the osteoclasts are involved in bone degeneration, while the osteocytes have a regulatory role. Misregulated bone remodelling will give altered bone density and

structure, resulting in osteoporosis. One option for treating the disease is to modulate the activity of osteoclasts. It has been found that CSF1R and RANKL mediated signalling are essential for osteoclast function, proliferation and differentiation [5,6]. Thus, situated at the beginning of the signalling cascade, CSF1R is an attractive target for controlling osteoclast activity and thereby treating osteoporosis. A current active field of research is the identification of selective CSF1R inhibitors, and the small molecular inhibitors GW2580 [7], PLX647 [8] and the most developed PLX3397 or *Pexidartinib* [9] have been found to down-regulate osteoclast activity in model systems.

The juxtamembrane (JM) is a flexible domain following the transmembrane loop [10]. For CSF1R and other platelet-derived growth factor (PDGF) family of receptors, JM greatly influences the activation state of the enzyme [11]. Through its interaction with the kinase domain, JM stabilizes the protein in an inactive, *autoinhibited* state [12,

* Corresponding author. Department of Chemistry, Norwegian University of Science and Technology, Høgskoleringen 5, NO-7491, Trondheim, Norway.
E-mail address: bard.helge.hoff@chem.ntnu (B.H. Hoff).

<https://doi.org/10.1016/j.ejmech.2023.115344>

Received 20 January 2023; Received in revised form 24 March 2023; Accepted 3 April 2023

Available online 28 April 2023

0223-5234/© 2023 The Authors. Published by Elsevier Masson SAS. This is an open access article under the CC BY license (<http://creativecommons.org/licenses/by/4.0/>).

13]. This autoinhibitory mechanism is also seen in Ephrin (Eph) and muscle-specific kinase (MUSK) receptors [11]. After phosphorylation and consequent undocking of the JM domain, a state referred to as *nonautoinhibited* is attained. Further, the activation loop can be phosphorylated to stabilize the enzyme in a fully active, catalytically competent DFG-in conformation. Hanson et al. performed hierarchical clustering analysis of binding affinity for 645 inhibitors towards 406 kinases [14]. This revealed CSF1R and others in the PDGF receptor family to be among the most promiscuous kinases, binding around five times as many ligands as the average kinase. The observation was explained by the relative high stability of the DFG-out, inactive conformation shared by these kinases. As a result, the PDGF family of kinases bind known Type I inhibitors in a DFG-out conformation normally observed for Type II inhibitors [12]. Further, analysis of kinase structures has revealed hydrophobic regions which is unique for the DGF-out conformation [15]. Such a small hydrophobic pocket has been the subject of attention in an inhibitor-design approach described as a new paradigm for discovery of inhibitors targeting the inactive, auto-inhibited conformation of protein kinases [15]. The pocket is distinct from the *allosteric back-pocket* targeted by traditional type II inhibitors such as Imatinib, GW2580 and PLX3397/Pexidartinib (Fig. 1).

Designing such type II inhibitors, typically requires substituents to interact with certain conserved elements of the allosteric back-pocket, such as the *gatekeeper residue* and the catalytic lysine, aspartic acid and glutamic acid residues. Although these interactions can yield potent inhibitors [16,17], the added chemical bulk of the introduced substituents might give rise to metabolic soft spots or toxic effects complicating drug development. We hypothesize that targeting the mentioned hydrophobic *front pocket* would give rise to atom efficient kinase inhibitors possessing unique properties with respect to selectivity and pharmaceutical behaviour.

Purines are an important class of heterocyclic structures [18–20] and is a frequently employed structural element in medicinal chemistry [21]. The purine scaffold has previously been applied in design of inhibitors for phosphatidylinositol-3-kinases [22], Src/Abl kinases [23], and glycogen synthase kinase [24]. However, there are no CSF1R inhibitors based on purines reported. Herein, we describe the structure-activity relationship (SAR) and initial ADME data on new purine-based CSF1R inhibitors having a potent down-regulating effect on osteoclast differentiation.

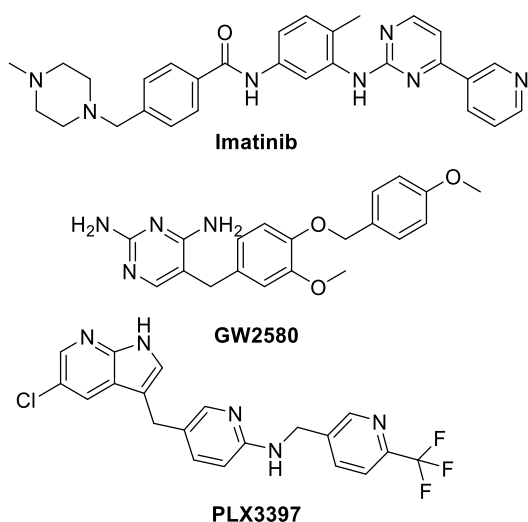


Fig. 1. Structures of CSF1R inhibitors Imatinib, GW2580 and PLX3397/Pexidartinib.

2. Results and discussion

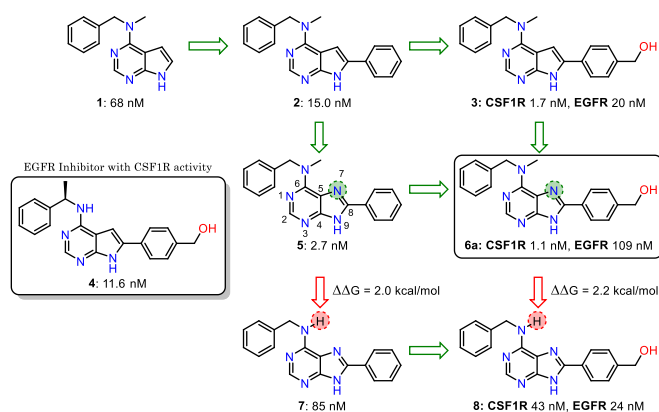
2.1. CSF1R inhibitory properties

In previously work we discovered inhibitors of the epidermal growth factor receptor (EGFR) with notable activity toward the CSF1R kinase [25]. In an effort to identify inhibitors with an improved CSF1R potency and selectivity profile, we synthesized simple derivatives of these parent pyrrolopyrimidines to establish key structural features required for activity. Initial findings showed that a simple scaffold hop from pyrrolopyrimidine to purine produced an increase in potency for a few simplified structures (Scheme 1). In addition, a significant boost in potency toward CSF1R, and simultaneous quenching of EGFR activity, was achieved by methylating the *N*-6' position (compound 5, Scheme 1). A comparison of CSF1R and EGFR inhibition data for these compounds is shown in the Supporting Information File (Table S1).

Molecular modelling studies indicated that this methyl is positioned in an appropriately sized, lipophilic pocket of the protein (Fig. 2). The increase in activity is higher than what would be expected by transferring a solvent-exposed methyl group on a ligand into a hydrophobic region of a protein (~2 kcal/mol vs. 0.7 kcal/mol) [26]. This suggests that the methyl group also contributes favourably through other mechanisms, such as conformational alignment or freeing of high energy waters near the binding pocket [27].

Encouraged by the strong effects of these simple substitutions, an expanded SAR study using 6-methylaminopurine as the core scaffold was initiated. From previous experience, the 4-hydroxymethylphenyl substituent had provided a marked improvement in activity toward CSF1R in biochemical assays for the pyrrolopyrimidines. A small panel of synthesized compounds also suggested this to be true for purines (compound 6a, Scheme 1). Choosing to keep this substituent as a base contributor to inhibitory activity, we focused our efforts on the *N*-6' amino substituent. Molecular docking experiments on a receptor grid generated from a CSF1R protein crystallized in the *DFG out*, auto-inhibited conformation (PDB ID: 6T2W) suggested that the *N*-6' substituent of compound 6a was placed in the hydrophobic pocket mentioned previously. To probe the nature of this somewhat close-fitting space of the protein, we synthesized a compound series containing simple chemical variations on the aromatic ring (Table 1). From these efforts, we observed only small differences in activity with methyl, fluoro and methoxy substituents in the *ortho*- and *meta*-positions.

Para-substitution appeared to have an undesirable effect on activity (compounds 6d, 6g and 6j) with the methoxy substituted analogue 6j being significantly less active at an IC_{50} of 61 nM. Much of the lost potency, however, could be restored by adding a *meta*-methoxy group (compound 6k, IC_{50} = 5.7 nM), suggesting some level of



Scheme 1. Effect of scaffold hopping from pyrrolopyrimidines to purines and simple purine decoration on CSF1R and EGFR inhibitory activity. The atom numbering of purines is shown for compound 5.

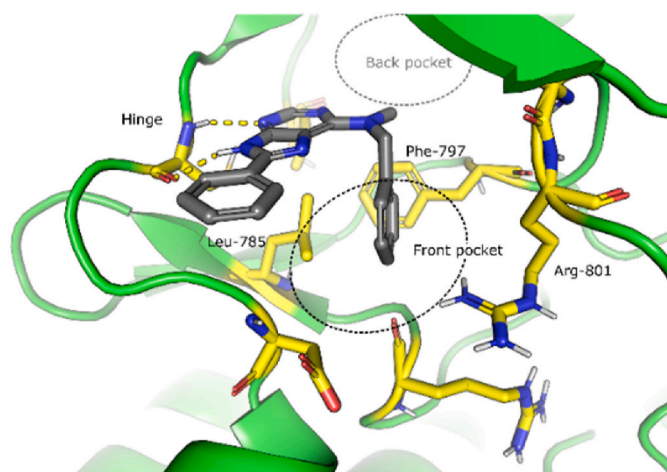


Fig. 2. The *N*-methyl group is placed in a small lipophilic pocket: 3D-model of compound **5** while docked in the active site of CSF1R. The yellow coloured dashed lines show hydrogen bonding interaction with the hinge region.

accommodation for larger *para*-substituents. Of the pyridyl containing compounds, **6n** with the nitrogen in the 4-position, was the most potent. Molecular modelling indicated that placing a hydrogen bond acceptor in the 4-position might be favourable because of interactions with the guanidine unit of Arg801. Further, it seemed like only *meta*-substitution by a methyl (compound **6c**) was tolerated in terms of retaining the activity of the unsubstituted parent compound. No clear difference in activity could be discerned between inhibitors bearing either electron rich or withdrawing aromatic substituents, indicating that only minor

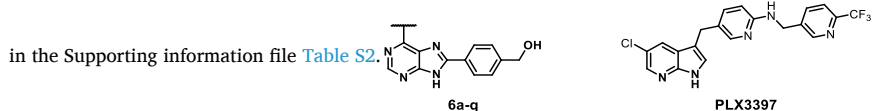
interactions between the π -cloud of the inhibitors and the protein is present. Seemingly limited by the positioning of the flat aromatic group within the binding pocket, we turned to aliphatic rings in hopes of slightly shifting the space-filling character of this substituent and arrange for more productive decorations. Molecular docking experiments supported these assumptions and proposed that the increased flexibility of the sp^3 -hybridized carbons allowed for more intimate contact between the substituent and the lipophilic environment formed by residues Phe797, Leu785, Ala800 and the aliphatic side chain of Arg801. The increased flexibility of the ligand simultaneously could allow the 4-hydroxymethylphenyl unit to be angled closer to the C-lobe and consequently engage in a hydrogen bonding interaction to Asp670 (Fig. 3).

We therefore made the saturated analogues **6r-y**. Of these, most were potent inhibitors in enzymatic assays. The cyclohexyl derivative **6s** had potency on par with its aromatic counterpart **6a**, while the cyclopentyl analogue **6r** exhibited sub-nanomolar enzymatic inhibition. A full-scale competitive binding assay panel screen on 468 kinases showed compound **6r** to have excellent selectivity for CSF1R (Fig. 4). Encouragingly, other members of the PDGF receptor family, wild type KIT (auto-inhibited), FLT3 (autoinhibited), PDGFR α and PDGFR β were only moderately inhibited (12–57% at 500 nM test concentration, see Supporting Information File, Table S5). However, FLT3 carrying the D835V mutation was bound more strongly (92%). Apart from CSF1R, the ABL1 H396P mutant had the highest affinity (96% bound), while of the non-mutants, EPHB6 (Ephrin type-B receptor 6) was highest (87% bound). EPHB6 is lacking kinase activity. Thus, it is unknown how the CSF1R inhibitors will affect its function. Ephrin type receptors have generally been recognized for their role in immune cell development [28] and elevated expression levels of EPHB6 are seen in some cancers [29–31].

A way of quantifying inhibitor selectivity, which assumes that low

Table 1

Effect of structural variations of purines on CSF1R inhibitory properties (IC_{50} , nM). PLX3397 was used as positive control. Examples of IC_{50} titration curves are shown



Comp.	Amine	Enzymatic CSF1R IC_{50} [nM] ^a	Comp.	Amine	Enzymatic CSF1R IC_{50} [nM] ^a
PLX3397	–	9.8	6m		3.8
6a		1.1	6n		2.2
6b		1.8	6o		2.3
6c		1.3	6p		11
6d		11	6q		2.9
6e		2.3	6r		0.5
6f		3.5	6s		1.0
6g		8.8	6t		2.6
6h		4.2	6u		4.6
6i		2.7	6v		1.3
6j		61	6w		0.3
6k		5.7	6x		53
6l		7.2	6y		130

^a Enzymatic inhibition assay was performed by 10-point titration using 3-fold serial dilutions from 1000 nM run in duplicates (20 data points).

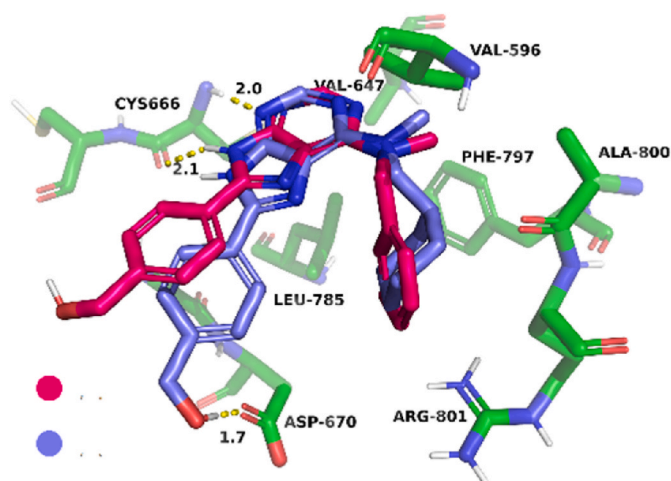


Fig. 3. Molecular docking indicated that the higher flexibility when introducing saturated amines (pink structure) allows for better contact between the 4-hydroxymethyl group and Asp670. Hydrogen bonding interactions are shown with yellow dashed lines.

inhibitory activity is clinically irrelevant, is the so-called selectivity score (S-score) [29]. It is calculated by dividing the number of kinases showing inhibition above a set limit by the total number of kinases evaluated. Thus, a non-selective inhibitor has a selectivity score close to unity, while a selective inhibitor has a score close to zero. Employing 50% inhibition as the threshold for the calculation, inhibitor **6r** has a S-score of 0.06, while using 30% the S-score was 0.31. Further on, we synthesized compounds **6t** - **6w** carrying tetrahydropyrans and tetrahydrofurans, indicated by molecular modelling to sit in the hydrophobic front pocket. Especially interesting was the pyran substituted **6v** and **6w** possessing both high activity and favourable solubility. The piperidine based compounds **6x** and **6y** had low enzymatic CSF1R activity.

2.2. Cell-based assays, ADME profile and pharmacokinetic studies

As an *in vitro* proxy for osteoporosis, we used CSF1 induced signalling in bone marrow-derived macrophages (BMDM) from mice femur. The effect of the inhibitors on CSF1R signalling was evaluated as activity of ERK1/2 measured as the level of the active, phosphorylated form of ERK1/2 (p-EKR1/2). The measurement was performed following 10 min treatment with or without CSF1 in the presence or absence of the respective inhibitors. This approach was chosen as tyrosine kinases receptors activates ERK1/2 more than other MAPK pathways, and since the use of p-CSF1R antibodies in our assay displayed a lower ability to discriminate between inactive (without CSF1 added) and active receptor (time-laps after CSF1 supplementation). PLX3397 was used as a reference. Due to some inter assay variation, activity relative to that of PLX3397 was found useful (fold change). Even though the inhibitor series containing aromatic amines (compounds **6a**-**6q**) had excellent enzymatic CSF1R IC_{50} values, only **6a** possessed measurable activity in the BMDM assay, **Table 2**. Mice BMDM assay of cyclopentyl derivative **6r** on the other hand showed inhibitory potency comparable to that of PLX3397 (**Table 2**). However, inhibitor **6r** had significant phase I metabolism in mouse liver microsomes (MLM) as well as poor kinetic solubility in an aqueous buffer solution. Although the compound had only moderate phase I metabolism in human liver microsomes (HML), anticipating complications from the poor solubility and low MLM stability in subsequent studies, we sought more soluble compounds for further drug development. The inhibitors containing oxygenated heterocycles (compounds **6t**-**6w**) showed an improved solubility over the carbon analogues **6r** and **6s** (**Table 2**). Unfortunately, **6t**-**6v** did not display any activity in BMDM assay.

However, the oxanyl-substituted analogue **6w** had both sufficient

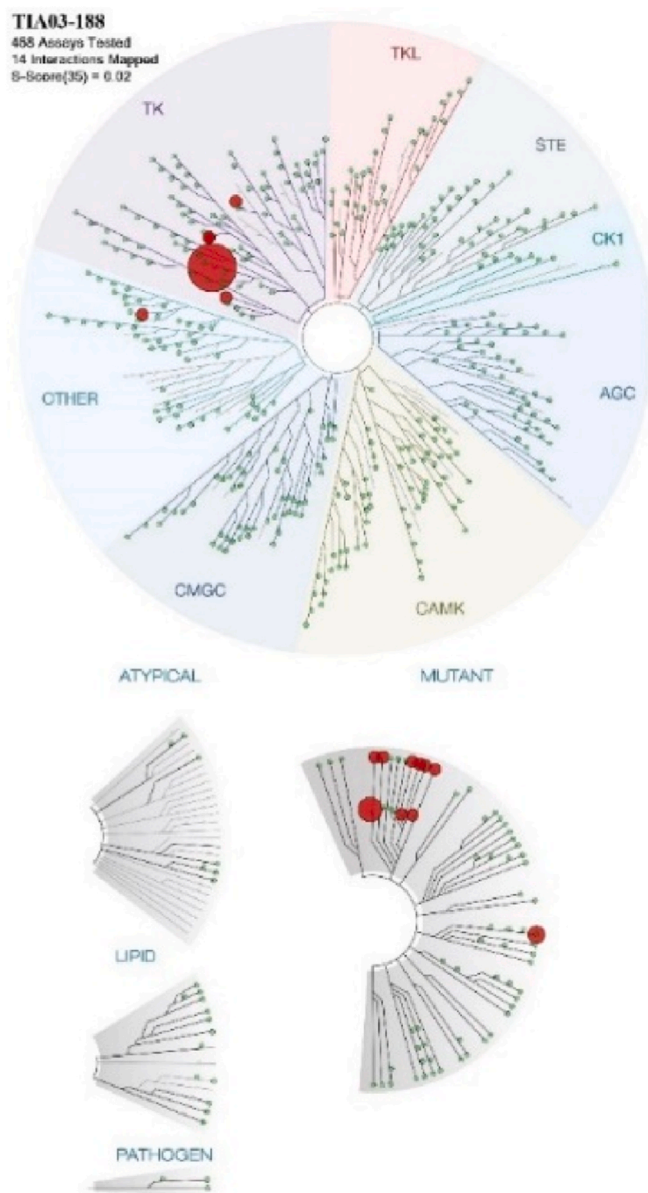
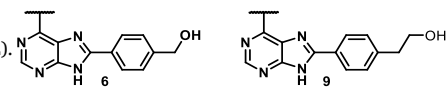


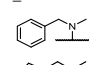
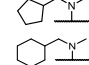
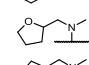
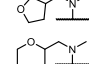
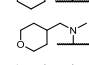
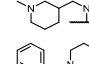
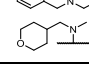
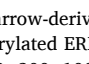
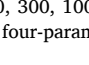
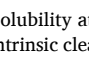
Fig. 4. Assay of compound **6r** towards a panel of 468 kinases at 500 nM represented with a kinome tree. Larger spheres indicate higher potency.

water solubility and high potency in the BMDM assay. Due to its promising properties, the oxanyl derivative **6w** was further evaluated *in vitro* and *in vivo*. Although compound **6w** had only somewhat elevated phase I metabolism in mouse liver microsomes, its stability in mouse hepatocytes was poor (**Table 3**). A mass spectroscopic stability study on compound **6w**, taking samples from the MLM mixture at timed intervals, indicated lability issues at the 4-hydroxymethylphenyl unit, stemming from oxidation of the benzylic carbon atom. Reasoning that such an oxidation might be impeded by homologation of the benzylic alcohol, compound **9** was synthesized (See **Table 2**). Indeed, its stability in mouse hepatocytes was considerably improved and enzymatic inhibitory potency was retained. With an IC_{50} of 0.2 nM in the ATP-based enzymatic assay, compound **9** is likely near the lower limit of sensitivity for this assay as a result of hitting the IC_{50} wall, the inherent limit encountered when reaching half the kinase test concentration. The calculated *binding efficiency index* (BEI) [32] of **9** based on the IC_{50} -value was 25.3, which is highly encouraging and indicate a very atom efficient binding. A screen towards a full panel of kinases confirmed that the high selectivity seen for **6v** was maintained in inhibitor **9** (**Fig. 5**). A good selectivity for

Table 2

Assays of selected purine CSF1R inhibitors towards mice BMDM, solubility, and phase I metabolism in mice liver microsomes (MLM) and human liver microsomes (HML).



Comp	Amine	BMDM		In vitro clearance	
		IC ₅₀ [nM] (fold of PLX3397) ^a	Solubility [μM] ^b	MLM [mL/ min/ μg] ^c	HLM [mL/ min/ μg] ^d
PLX3397	–	100–152 (1)	20.7	41.4	11.8
6a		330 (2.9)	–0.2	57.8	14.4
6r		40 (0.4)	3.5	243	36.4
6s		100 (0.9)	0.5	ND ^e	22.3
6t		>300	39.7	ND ^e	33.2
6u		>300	131	ND ^e	20.1
6v		>300	9.2	ND ^e	24.2
6w		83 (0.9)	55.4	58.7	15.8
6x		>300	469	ND ^e	3.6
6y		>300	33.5	ND ^e	22.1
9		106 (0.7)	37.5	30.2	14.7

^a Bone marrow-derived macrophages (BMDM) isolated from mice measured for phosphorylated ERK1/2. The experiment was run at five inhibitor concentrations: 500, 300, 100, 50, 10 nM. The data was normalized to expressed p-ERK1/2 and four-parameter logistic dose-response curves were fitted to the data points.

^b Kinetic solubility at pH 7.4.

^c In vitro intrinsic clearance of compounds in mouse liver microsome (MLM) – Phase I.

^d In vitro intrinsic clearance of compounds in human liver microsome (HLM) – Phase I.

^e Not determined.

CSF1R towards the other RKT-III family kinases was seen (Table S5, Supporting information File). The S-score at 50% inhibition was 0.06, while at 30% it was as 0.11. Further, inhibitor **9** was equipotent to PLX3397 in mice BMDM assay (see Fig. 6).

Further, inhibitor **9** was compared with **6w** and PLX3397 in an osteoclast differentiation assay. Human osteoclast precursor cells were stimulated for seven days with CSF1 and RANKL at 0.01–1000 nM

concentrations of the inhibitors. The experiment showed a complete suppression of osteoclast formation at 1000 and 100 nM as judged by microscopic imaging (osteoclast count) and measurement of tartrate-resistant acid phosphatase (TRAP) activity in the supernatant. At 10 nM concentration, the phenotype of the inhibitor-treated cells matched that of the CSF1 negative control, see Fig. 7. Representative immunofluorescence images are shown in Table S7. The high selectivity of compound **6w** and **9** suggest the effect is mediated by CSF1R inhibition and not through any kinase off-target contributions.

However, it is surprising that even though compounds **6w** and **9** were found more potent in enzymatic assays, PLX3397 is more efficient in suppressing osteoclast differentiation. To investigate this phenomenon compounds **6w**, **9** and PLX3397 were assayed for their ability to suppress proliferation of CSF1R engineered Ba/F3 cells. PLX3397 was found to be far more potent with an IC₅₀ of 0.06 μM, while **6w** and **9** had IC₅₀ of 3.1 μM and 1.5 μM, respectively (Table S8, Supporting Information File). Possible reasons for this behaviour could be permeability issues like high efflux, that the inhibitors are outcompeted by the higher ATP concentration in the cell assay, or that the compounds inhibit an irrelevant form of CSF1R (see section below).

In vivo single dose pharmacokinetics of **6w**, **9** and PLX3397 was performed by IV cassette dosing (1 mg/kg pr drug) in C57BLKS, female mice. The stability of the two front runner candidates largely followed the trend shown from the hepatocyte assay with a 10-fold higher clearance for **6w** as compared to **9**. However, when comparing with the stability data of PLX3397, it is clear further tuning of stability is needed to proceed with efficacy studies in mice.

2.3. Mode of action

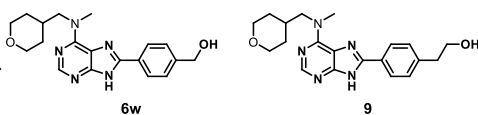
To further investigate the compounds mode of action inhibitors **6r**, **6w** and **9** were profiled in assays representing the autoinhibited and non-autoinhibited form of the kinase. The dissociation constants (K_d) are compared with that of PLX3397 in Table 4.

All three compounds bind strongly to the autoinhibited form of the kinase, with an 18- and 72-fold preference over the non-autoinhibited form for compound **6w** and **9** respectively. This validates the choice of protein construct (DFG-out, JM domain present and docked) used in our molecular modelling studies. The docked pose of inhibitor **9** in CSF1R is shown in Fig. 8.

According to this model the purine N-3 and NH-9 are involved in hydrogen bonding with the hinge residue Cys-666. Further, the pyran unit both possesses lipophilic interactions, and the oxygen is assumed to accept a hydrogen bond from Arg-801. The N-methyl groups occupies a lipophilic cavity of limited size. The aryl group extending from C-8 obviously has lipophilic interactions, but also places the hydroxyethyl

Table 3

Pharmacokinetic data for compounds **6w** and **9**.



Comp.	In vitro				In vivo		
	PPB [%] ^a	Plasma stab. ^b [%] ^b	Microsomal stab phase II [%] ^c	Hepatocyte CL _{int} [μL/min/10 ⁶ cells] ^d	t _{1/2} [h] ^e	CL ^f [L/h/kg]	V _{ss obs} [L/kg] ^g
6w	56	100	83	148	0.4	198	80
9	63.4	97.9	97.2	22	0.4	19	9
PLX3397	99.3	100	69	ND ^h	5.6	0.05	0.4

^a Mouse plasma protein binding, fraction bound.

^b Mouse plasma stability, remaining compound (%) at 5 μM concentration.

^c Mouse microsomal stability, phase II metabolism, remaining compound (%) at 5 μM concentration.

^d Intrinsic clearance in mouse hepatocytes.

^e In vivo half-life in C57BLKS, female mice (n = 3) by IV (1 mg/kg).

^f In vivo clearance in C57BLKS, female mice (n = 3) by IV (1 mg/kg).

^g Steady state volume of distribution in C57BLKS, female mice (n = 3) by IV (1 mg/kg).

^h Not determined.

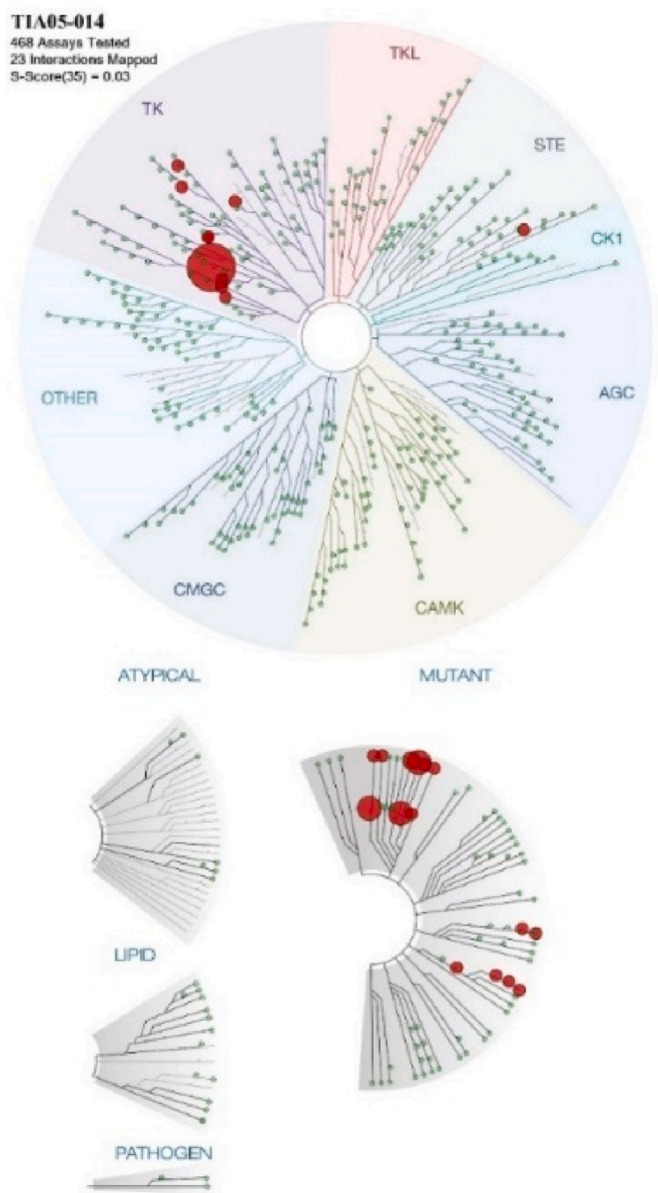


Fig. 5. Assay of compound **9** towards a panel of 468 kinase at 500 nM represented with a kinome tree. Larger spheres indicate higher potency.

group in correct position for participation in a hydrogen bonding network with Asn-673 and Asp-670. The preference for the autoinhibited form is opposite to that of other known CSF1R inhibitors such as GW-2580, Dasatinib, Imatinib, Ki-20227 [12] and our benchmark reference PLX3397. This distinctive feature may explain the observed selectivity profile of compounds **6r** and **9** as a consequence of targeting a narrower subset of kinase forms. Indeed, FLT3, EphB6 and KIT kinases, all harbouring autoinhibitory JM domains, have some affinities toward compound **9**. TYK2, a Janus kinase containing an autoinhibitory *pseudokinase* domain which may function through similar interactions to that of the Eph and PDGF receptors [33], also possesses affinity to the tested compounds. As indicated by our molecular modelling studies, it seems compound **9** takes advantage of this unique structural unit, having its cyclic amine-substituent placed in the shielded environment provided by the activation loop in the DFG-out conformation. It is reported that for Abl kinases, this hydrophobic shielding can also be realized through the action of its P-loop. When folding over the bound ligand, the P-loop shields it from the solvent in the DFG-in conformation [14], a seemingly rare property among kinases [34]. This behaviour may

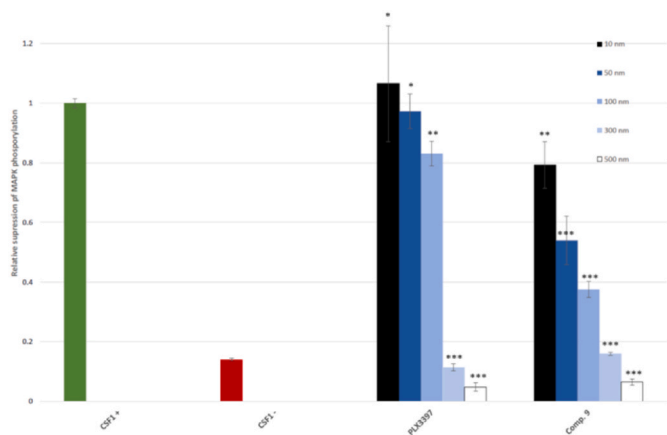


Fig. 6. Downstream p-ERK1/2 signalling effect of inhibitor **9** compared to PLX3397 in mice BMDM. The relative level of phosphorylated ERK1/2 is shown in the presence of CSF1 (green), without CSF1 (red) and in the presence of various concentrations of the inhibitors PLX3397 and **9**. The cell assay is based on triplicate measurements. Statistical significance was calculated by unpaired two-tailed Student's *t*-test comparing each test concentration with untreated using SigmaPlot 14.0: ****P* < 0.001, ***P* < 0.05, **P* > 0.49.

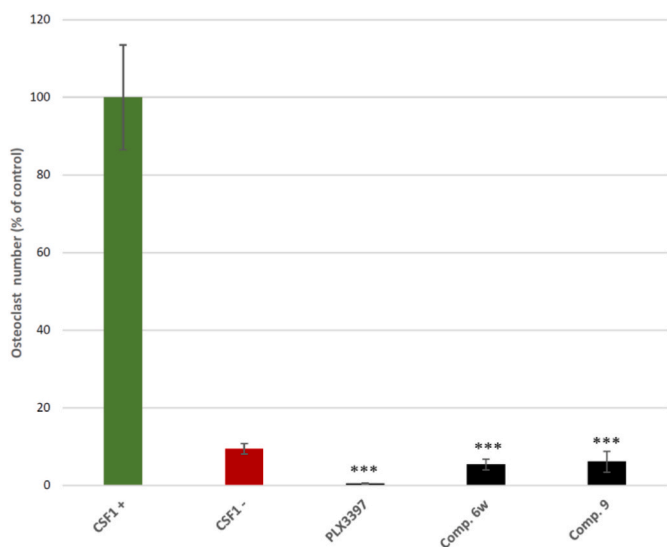


Fig. 7. Effect of inhibitor **6w**, **9** and PLX3397 on osteoclast count at 10 nM concentration. Statistical significance was calculated by unpaired two-tailed Student's *t*-test comparing each test concentration with untreated using SigmaPlot 14.0: ****P* < 0.006.

Table 4

Dissociation constants (K_d) measured against the autoinhibited and non-autoinhibited form of CSF1R.^a

Comp.	Autoinhibited K_d [nM]	Nonautoinhibited K_d [nM]
PLX3397	360	5.8
6r	17	220
6w	4.5	80
9	0.5	36

^a Dissociation constants calculated using the Hill-equation. Data points were curve-fitted from 11-point, 3-fold serial dilution sampling measurements. The titration curves are shown in the Supporting information file, Tables S3 and S4.

explain the binding affinities toward the various Abl mutants observed for compounds **6w** and **9**. It remains to see if antagonists towards the autoinhibited form of CSF1R is of medicinal importance. Anyhow,

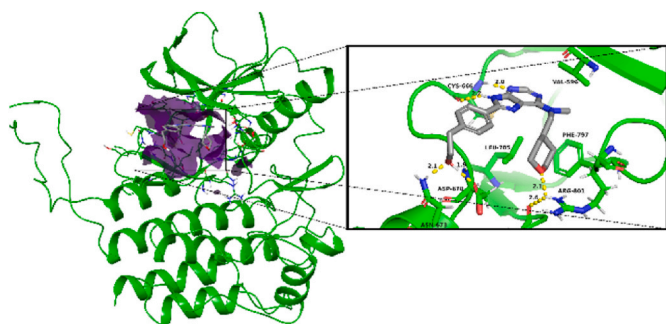


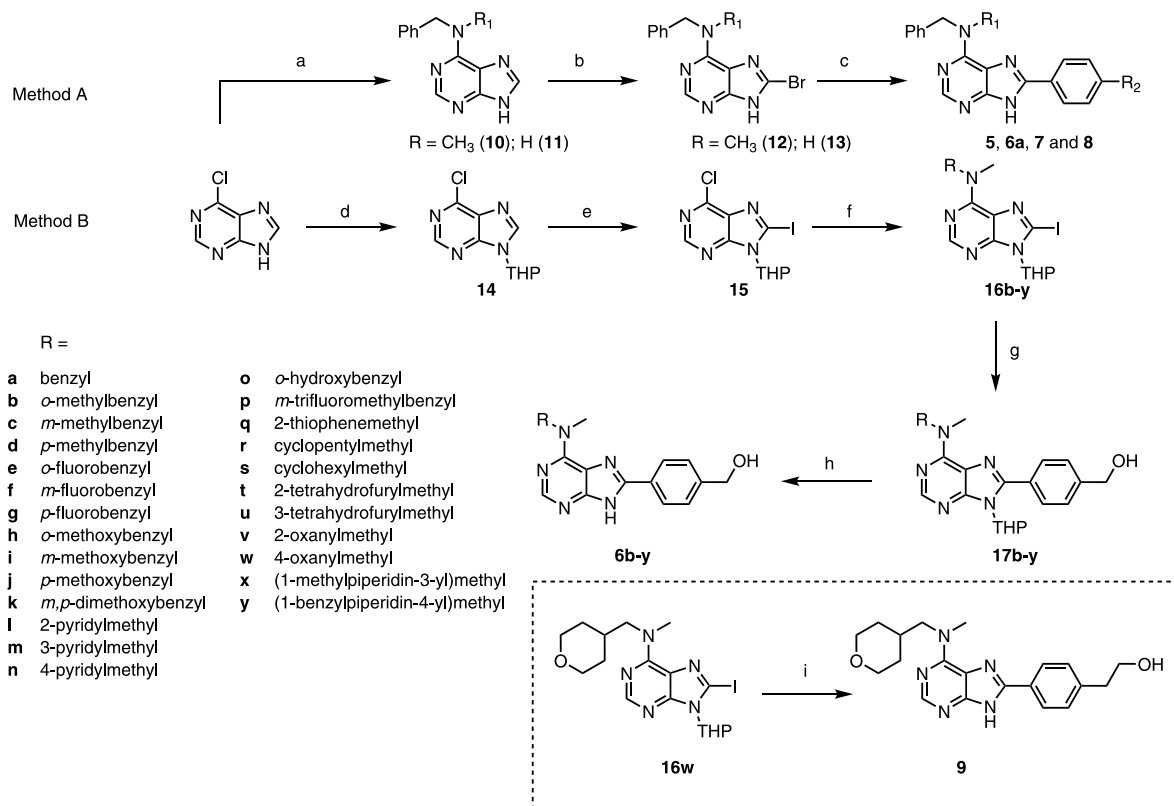
Fig. 8. Proposed binding mode of inhibitor **9**. Hydrogen bonding interactions are shown with yellow dashed lines.

having tool compounds as **9** available, can be important to broaden knowledge.

2.4. Chemistry

The initial method used to prepare the inhibitor structures are shown in **Scheme 2** (Route A). Starting from commercially available 6-chloropurine the C-6 aminated products **10** and **11** were formed. These were then brominated at C-8 to yield **12** and **13** in mediocre yields. Subsequently, Suzuki-Miyaura cross-couplings and purification gave compounds **5**, **6a**, **7** and **8**. However, with the need to repeat the rather low yielding bromination for each new amine introduced, the above method is rather inconvenient when a compound collection is to be made. Instead (Method B, **Scheme 2**), 6-chloropurine (**2**) was selectively

protected at the N-9 nitrogen roughly following literature procedures using the tetrahydropyran protecting group [35]. Iodination of the C-8 position in **14** was done at $-78\text{ }^{\circ}\text{C}$ in a two-step lithiation-halogenation reaction using lithium diisopropylamide (LDA) as base and elemental iodine. The protected 4-chloro-8-iodo-purine **15**, prepared in 10 g scale (74% yield), served as a late-stage precursor for substitution of the purine scaffold. Exploiting the electron deficient nature of this heterocyclic ring system, nucleophilic aromatic substitution on **15** was readily carried out under mild conditions using a slight excess of the N-methylated amine together with at least one equivalent of a non-nucleophilic amine co-base such as triethylamine or diisopropylethylamine. At $50\text{ }^{\circ}\text{C}$, the substitution requires reaction times in excess of 200 min to reach full conversion of the starting material. Running the reaction at $70\text{ }^{\circ}\text{C}$, full conversion is typically reached after 90 min. Using ether solvents such as 1,4-dioxane or THF, in many cases we observed precipitation of triethylammonium chloride from the reaction mixture, which may have helped drive the reaction to completion more quickly. Subsequent Suzuki-Miyaura cross-coupling reactions on the 6-amino-8-iodo-purines **16b-y** to introduce the 4-hydroxymethylphenyl group on C-8, was found to proceed rapidly at $80\text{ }^{\circ}\text{C}$ using a range of palladium catalysts. Pd-PEPPSI-SIPr and PdCl₂(dppf) are preferred catalysts. The side reactions observed in the cross-coupling reaction was oxidation of the hydroxymethyl unit into the corresponding benzaldehyde as well as dehalogenation of the starting substrate. Prior to purification the by-products were rarely present at more than 3 mol% relative to the product. Due to their differences in polarity, these by-products could be separated from the product through simple chromatographic means. Cleavage of the THP-protection group on compounds **17b-y**, was facile under several reaction conditions. Refluxing in an alcoholic solvent



Scheme 2. Synthesis of compounds **6a-y** and **9**. Reagents and conditions: (a) Benzylamine, diisopropylethylamine, *n*-BuOH or 1,4-dioxane, Δ , 2–20 h, 82–93%; (b) Br₂, AcOH, NaOAc, 22–24 h, 44–47%; (c) Arylboronic acid, Pd-PEPPSI-SIPr or XPhos Pd G2, K₂CO₃, 1,4-dioxane, H₂O, 100 $^{\circ}\text{C}$, 17–87%; (d) Benzylamine, 3,4-dihydro-2H-pyran, *p*-TsOH•H₂O, EtOAc, 90 $^{\circ}\text{C}$, 97%; (e) Lithium diisopropylamide (LDA), I₂, THF, $-78\text{ }^{\circ}\text{C}$, 77%; (f) R-substituted methylamine, triethylamine or diisopropylethylamine, 1,4-dioxane, 70 $^{\circ}\text{C}$, 70–94%; (g) 4-Hydroxymethylphenyl boronic acid, PdCl₂(dppf) or Pd-PEPPSI-SIPr, K₂CO₃, 1,4-dioxane, H₂O, 80 or 100 $^{\circ}\text{C}$, 63–95%; (h) *p*-TsOH•H₂O, MeOH, reflux or hydrochloric acid, EtOH, rt, 77–94%; (i) 1. (4-(2-Hydroxyethyl)phenyl)boronic acid, PdCl₂(dppf), K₂CO₃, dioxane/water, 2:1, 80 $^{\circ}\text{C}$, 2. HCl, MeOH, 70 $^{\circ}\text{C}$, 84%.

(MeOH, EtOH or *i*-PrOH) with catalytic amounts of acid (*p*-TsOH, hydrochloric acid), yielded the deprotected final products **6b-y** with minimal by-product formation. Compound **9** was made with the same strategy starting from **16w**. Significant band broadening for proton and carbon NMR signals originating from the N-CH₃ and N-CH₂- groups were seen. These signals are sharpened by running the NMR experiments at 75 °C, see Supporting information File.

3. Conclusion

Through a scaffold-hopping exercise and a systematic SAR study, we have discovered a highly potent CSF1R purine inhibitor **9** displaying high selectivity across the human kinome. The inhibitor binds preferentially to the *autoinhibited* form of the kinase, in contrast to that observed for other reported inhibitors of CSF1R. Molecular modelling indicate the inhibitor targets a hydrophobic pocket formed by Phe-797, Leu-785, Ala-800 and Arg-801 of the kinase in the inactive state, a region not typically targeted by type II inhibitors. The exceptionally high *binding efficiency index* (BEI) of **9** demonstrates the lean but potent nature of this class of inhibitors, and provides leeway for synthetic optimization in subsequent stages of the drug development process, potentially minimizing the risk of attrition [36]. Inhibitor **9** attenuates the phosphorylation of downstream MAPK/ERK receptors in mice bone marrow derived macrophages at similar concentrations to the approved drug PLX3397. The inhibitor also prevents maturation of osteoclasts from RANKL and CSF1 stimulated osteoclast precursor cells. The medicinal relevance of blocking the *autoinhibited* form of CSF1R remains to be revealed. The purine inhibitor **9** might in this respect be a very important tool compound.

4. Experimental

4.1. General

6-Chloro-9-(tetrahydropyran-2-yl)-9H-purine was ordered from abcr GmbH. Dry solvents were collected from a Braun MB SPS-800 solvent purification system. The synthesis of compound **2** and **3** will be disclosed elsewhere, while preparation of **4** is described in Kaspersen et al. [25] All other reagents, starting materials and solvents were purchased from Sigma-Aldrich and used as is. Reactions were monitored by thin-layer chromatography (TLC) using silica-gel on aluminium plates, F254, Merck. Purification of compounds by flash column chromatography was performed on pre-packaged silica-gel cartridges obtained from Interchim (PuriFlash cartridges) or with silica-gel (40–63 mesh, 60 Å) using standard glass-ware. NMR spectra were recorded on a Bruker Avance III HD 400 or 600 MHz instrument in either CDCl₃ containing tetramethylsilane or DMSO-*d*₆ as solvents. ¹H and ¹³C chemical shifts are reported in part per million (ppm, δ) using tetramethylsilane (0.00 ppm) or residual solvent (DMSO-*d*₅, 2.50/39.52 ppm) as internal reference standard. Infrared absorption spectra were recorded on a Thermo Nicolet Nexus FT-IR spectrometer using a Smart Endurance reflection cell. Absorption bands are reported as strong (s), medium (m) or weak (w). Accurate mass determination was performed on a Synapt G2-S Q-TOF instrument from Waters TM in either positive or negative mode. The samples were ionized with an ASAP (APCI) or ESI probe. Exact mass calculations and spectra processing was done using Waters TM Software Masslynx V4.1 SCN871. The purity of the final inhibitors was assessed on an Agilent 1100-series modular HPLC instrument with a diode array detector using a C-18 Poroshell 120 (100 × 4.6 mm, 2.7 μm) column. The spectra were recorded and analysed at 254 nm and processed using Agilent ChemStation software.

5. Synthesis

5.1. General Procedure 1 – thermal nucleophilic amination

6-Chloro-8-iodo-9-(tetrahydro-2H-pyran-2-yl)-9H-purine (1.0 equiv.), triethylamine (1.5 equiv.) or *N,N*-diisopropylethylamine (1.5 equiv.) and the appropriate amine nucleophile (1.5 equiv.) was dissolved in 1,4-dioxane (7.5 mL/mmol). The reaction mixture was lowered into an oil-bath set at 70 °C and stirred. Upon reaction completion, the reaction vessel was raised from the oil-bath and allowed to cool for 5 min before the volatiles were removed in vacuo. The residue was added water (10 mL) and extracted with DCM (3 × 10 mL). The combined organic layers were washed with brine (10 mL), dried over anhydrous Na₂SO₄ and filtered. The organic solvent was removed under reduced pressure and the crude product was purified by silica-gel column chromatography. The solvent systems used are specified for each compound.

5.2. General Procedure 2 – Suzuki-Miyaura cross coupling reaction

Starting material (1.0 equiv.), boronic acid (1.2 equiv.), palladium catalyst (5 mol%) and potassium carbonate (3.0 equiv.) was charged in a Schlenk tube. The atmosphere was evacuated and back-filled with N₂ three times before adding 1,4-dioxane and water. The reaction mixture was lowered into an oil-bath set at 80 or 100 °C and stirred vigorously. Upon reaction completion, the Schlenk tube was raised from the oil-bath and allowed to cool for 5 min before the reaction mixture was transferred to a round-bottomed flask and the volatiles removed by rotary evaporation. The residue was added water (10 mL) and extracted with DCM (3 × 10 mL). The combined organic layers were washed with brine (10 mL), dried over anhydrous Na₂SO₄ and filtered. The organic solvent was removed under reduced pressure and the crude product was purified by silica-gel column chromatography. The solvent systems used are specified for each compound.

5.3. General Procedure 3 – THP deprotection

THP-protected starting material (1.0 equiv.) and *para*-toluenesulfonic acid monohydrate (5 mol%) was dissolved in MeOH (10 mL/mmol) and the reaction mixture was lowered into an oil-bath set at 70 °C and stirred. In some cases Amberlyst 15 in MeOH at 70 °C or aqueous HCl (37%) in EtOH at 0 °C were used. Upon reaction completion, the reaction vessel was raised from the oil-bath and allowed to cool for 5 min before the reaction mixture was transferred to a round-bottomed flask and added a mixture of DCM and MeOH (~1:1) until all precipitated material had dissolved. To the solution, Celite (10:1 - Celite to starting material, by weight) was added and the volatiles were removed in vacuo. The dry residue was applied to a silica gel column for chromatographic purification. The solvent systems used are specified for each compound.

5.4. *N*-Benzyl-*N*-methyl-8-phenyl-9H-purin-6-amine (**5**)

The compound was synthesized according to General Procedure 2 using the bromide **13** (23 mg, 0.072 mmol), phenylboronic acid (13 mg, 0.108 mmol), Pd-PEPPSI-SIPr (2.5 mg, 0.0037 mmol) and K₂CO₃ (30 mg, 0.218 mmol) in 1,4-dioxane (0.655 mL) and water (0.655 mL). The reaction was stirred on an oil-bath (100 °C) for 1 h 40 min. Purification by silica-gel flash column chromatography (DCM/MeOH – 98:2) gave 20 mg (0.062 mmol, 86%) of a colourless solid. ¹H NMR (400 MHz, DMSO-*d*₆) δ 13.54 (br s, 1H), 8.25 (s, 1H), 8.15–8.08 (m, 2H), 7.54–7.44 (m, 3H), 7.35–7.29 (m, 4H), 7.29–7.22 (m, 1H), 5.45 (br s, 2H), 3.43 (br s, 3H); ¹³C NMR (101 MHz, DMSO-*d*₆) δ 153.7, 152.9, 152.0, 147.1, 129.9, 129.5, 128.9 (2C), 128.5 (2C), 127.5 (2C), 127.1, 126.1 (2C), 119.9, not detected at 25 °C: NCH₂C, NCH₃; HRMS (ES+, *m/z*): found 316.1565, calcd for C₁₉H₁₈N₅ [M+H]⁺ 316.1562.

5.5. (4-(6-(Benzyl(methyl)amino)-9H-purin-8-yl)phenyl)methanol (6a)

The compound was synthesized according to General Procedure 2 using the bromide **12** (51 mg, 0.160 mmol), 4-(hydroxymethyl)phenylboronic acid (37 mg, 0.242 mmol), Pd-PEPPSI-SIPr (5.6 mg, 0.0082 mmol) and K_2CO_3 (66 mg, 0.480 mmol) in 1,4-dioxane (1.45 mL) and water (1.45 mL). The reaction was stirred on an oil-bath (100 °C) for 2 h. Purification by silica-gel flash column chromatography (DCM/MeOH – 97:3) gave 48 mg (0.140 mmol, 87%) of a colourless solid, mp. >250 °C (decomp.). 1H NMR (600 MHz, DMSO- d_6) δ 13.49 (s, 1H), 8.24 (s, 1H), 8.09–8.05 (m, 2H), 7.47–7.42 (m, 2H), 7.36–7.29 (m, 4H), 7.29–7.22 (m, 1H), 5.29 (t, $J = 5.7$ Hz, 1H), 4.55 (d, $J = 5.6$ Hz, 2H), not detected at 25 °C: NCH_2 , NCH_3 ; ^{13}C NMR (151 MHz, DMSO- d_6) δ 153.6, 152.8, 151.9, 147.2, 144.5, 138.3, 128.5 (2C), 127.9, 127.5 (2C), 127.0, 126.8 (2C), 125.9 (2C), 119.9, 62.5, 52.7, 35.6; HRMS (ES+, m/z): found 351.2184, calcd for $C_{21}H_{27}N_4O$ $[M+H]^+$ 351.2185.

5.6. N-methyl-N-(2-methylbenzyl)-8-(4-(hydroxymethyl)phenyl)-9H-purin-6-amine (6b)

The compound was synthesized according to General Procedure 3 using **17b** (42.7 mg, 0.096 mmol). The reaction time was 2.75 h. Purification by silica-gel flash column chromatography (DCM/MeOH (sat. w/ NH_3) – 9:1, $R_f = 0.36$) gave 26.8 mg (0.082 mmol, 77%) of a colourless solid, mp > 300 °C. 1H NMR (600 MHz, DMSO- d_6) δ 13.45 (s, 1H), 8.22 (s, 1H), 8.07–8.03 (m, 2H), 7.46–7.42 (m, 2H), 7.23–7.19 (m, 1H), 7.17–7.13 (m, 1H), 7.13–7.09 (m, 1H), 7.06–7.01 (m, 1H), 5.37 (br s, 2H), 5.28 (t, $J = 5.7$ Hz, 1H), 4.55 (d, $J = 5.5$ Hz, 2H), 3.42 (br s, 3H), 2.33 (s, 3H); ^{13}C NMR (151 MHz, DMSO- d_6) δ 153.8, 152.8, 151.9, 147.1, 144.5, 135.9, 135.8, 130.2, 127.9, 126.7 (2C), 126.2, 125.92, 125.89 (2C), 119.9, 62.5, 18.8, not detected at 25 °C: NCH_2 , NCH_3 ; IR (neat, cm^{-1}): 3304 (br w), 3097 (w), 3061 (w), 3017 (w), 2957 (w), 2868 (w), 2832 (w), 2724 (w), 2696 (w), 1589 (s), 1521 (m), 1441 (m), 1401 (m), 1326 (m), 1306 (m), 1054 (m), 950 (m), 836 (m), 742 (m), 725 (m), 679 (m); HRMS (ASAP+, m/z): found 360.1826, calcd for $C_{21}H_{22}N_5O$ $[M+H]^+$ 360.1824.

5.7. N-methyl-N-(3-methylbenzyl)-8-(4-(hydroxymethyl)phenyl)-9H-purin-6-amine (6c)

The compound was synthesized according to General Procedure 3 using **17c** (35.5 mg, 0.080 mmol). The reaction time was 4 h. Purification by silica-gel flash column chromatography (DCM/MeOH – 19:1, $R_f = 0.16$) gave 25.4 mg (0.071 mmol, 88%) of a colourless solid, mp. 263–264 °C. 1H NMR (600 MHz, DMSO- d_6) δ 13.47 (s, 1H), 8.23 (s, 1H), 8.09–8.05 (m, 2H), 7.47–7.42 (m, 2H), 7.23–7.18 (m, 1H), 7.14 (s, 1H), 7.11–7.05 (m, 2H), 5.44 (br s, 2H), 5.28 (t, $J = 5.7$ Hz, 1H), 4.55 (d, $J = 5.5$ Hz, 2H), 3.43 (br s, 3H), 2.26 (s, 3H); ^{13}C NMR (151 MHz, DMSO- d_6) δ 153.6, 152.8, 151.9, 147.1, 144.5, 138.2, 137.6, 128.4, 128.0, 127.9, 127.7, 126.8 (2C), 125.9 (2C), 124.5, 119.9, 62.5, 21.1, not detected at 25 °C: NCH_2 , NCH_3 ; IR (neat, cm^{-1}): 3302 (br w), 3096 (w), 3027 (w), 2920 (w), 2868 (w), 2694 (w), 1592 (s), 1538 (m), 1521 (m), 1441 (m), 1404 (m), 1326 (m), 1315 (m), 1048 (m), 951 (m), 842 (m), 727 (m), 690 (m), 680 (m); HRMS (ASAP+, m/z): found 360.1825, calcd for $C_{21}H_{22}N_5O$ $[M+H]^+$ 360.1824.

5.8. N-methyl-N-(4-methylbenzyl)-8-(4-(hydroxymethyl)phenyl)-9H-purin-6-amine (6d)

The compound was synthesized according to General Procedure 3 using **17d** (23.9 mg, 0.054 mmol). The reaction time was 2 h. Purification by silica-gel flash column chromatography (DCM/MeOH – 19:1, $R_f = 0.45$) gave 17.3 mg (0.048 mmol, 89%) of a colourless solid, mp. 270–278 °C. 1H NMR (600 MHz, DMSO- d_6) δ 13.48 (s, 1H), 8.23 (s, 1H), 8.09–8.05 (m, 2H), 7.46–7.42 (m, 2H), 7.23–7.18 (m, 2H), 7.15–7.10 (m, 2H), 5.53 (br s, 2H), 5.29 (t, $J = 5.7$ Hz, 1H), 4.55 (d, $J = 5.6$ Hz,

2H), 3.23 (br s, 3H), 2.26 (s, 3H); ^{13}C NMR (151 MHz, DMSO- d_6) δ 153.6, 152.8, 151.9, 147.1, 144.5, 136.1, 135.2, 129.1 (2C), 128.0, 127.5 (2C), 126.8 (2C), 125.9 (2C), 119.9, 62.5, 20.7, not detected at 25 °C: NCH_2 , NCH_3 ; IR (neat, cm^{-1}): 3294 (br w), 3093 (w), 3010 (w), 2956 (w), 2923 (w), 2870 (w), 2829 (w), 2725 (w), 2692 (w), 1593 (s), 1518 (m), 1434 (m), 1403 (m), 1309 (m), 1051 (m), 949 (m), 840 (m), 796 (m), 789 (m), 725 (m), 681 (m), 468 (m); HRMS (ASAP+, m/z): found 360.1823, calcd for $C_{21}H_{22}N_5O$ $[M+H]^+$ 360.1824.

5.9. N-methyl-N-(2-fluorobenzyl)-8-(4-(hydroxymethyl)phenyl)-9H-purin-6-amine (6e)

The compound was synthesized according to General Procedure 3 with Amberlyst 15 using **17e** (29.9 mg, 0.067 mmol) and Amberlyst 15 (45 mg). The oil-bath temperature was set to 65 °C and the reaction time was 1 h. Purification by silica-gel flash column chromatography (DCM/MeOH - 9:1, $R_f = 0.37$) gave 3.7 mg (0.010 mmol, 15%) of a colourless powder. 1H NMR (600 MHz, DMSO- d_6) δ 13.36 (s, 1H), 8.24 (s, 1H), 8.09–8.04 (m, 2H), 7.46–7.42 (m, 2H), 7.34–7.29 (m, 1H), 7.29–7.24 (m, 1H), 7.25–7.19 (m, 1H), 7.15–7.10 (m, 1H), 5.56 (br s, 2H), 5.29 (t, $J = 5.7$ Hz, 1H), 4.55 (d, $J = 5.5$ Hz, 2H), 3.40 (br s, 3H); ^{13}C NMR (151 MHz, DMSO- d_6) δ 160.5 (d, $^1J_{CF} = 244$ Hz, 1C), 153.6, 152.9, 151.8, 147.3, 144.5, 129.04, 129.01, 128.98, 128.0, 126.7 (2C), 125.9 (2C), 124.6 (d, $^4J_{CF} = 3.3$ Hz, 1C), 120.0, 115.3 (d, $^2J_{CF} = 21.4$ Hz, 1C), 62.5, not detected at 25 °C: NCH_2 , NCH_3 ; HRMS (ASAP+, m/z): found 364.1576, calcd for $C_{20}H_{19}N_5OF$ $[M+H]^+$ 364.1574.

5.10. N-methyl-N-(3-fluorobenzyl)-8-(4-(hydroxymethyl)phenyl)-9H-purin-6-amine (6f)

The compound was synthesized according to General Procedure 3 with Amberlyst 15 using **17f** (55.0 mg, 0.067 mmol) and Amberlyst 15 (78 mg). The oil-bath temperature was set to 65 °C and the reaction time was 1 h. Purification by silica-gel flash column chromatography (DCM/MeOH - 92.5 : 7.5, $R_f = 0.21$) gave 9.3 mg (0.026 mmol, 21%) of a colourless powder. 1H NMR (600 MHz, DMSO- d_6) δ 13.50 (s, 1H), 8.24 (s, 1H), 8.10–8.05 (m, 2H), 7.47–7.42 (m, 2H), 7.41–7.34 (m, 1H), 7.18–7.12 (m, 2H), 7.12–7.05 (m, 1H), 5.46 (br s, 2H), 5.29 (t, $J = 5.7$ Hz, 1H), 4.55 (d, $J = 5.6$ Hz, 2H), 3.41 (br s, 3H); ^{13}C NMR (151 MHz, DMSO- d_6) δ 162.3 (d, $^1J_{CF} = 243.7$ Hz, 1C), 153.5, 153.0, 151.8, 147.4, 144.5, 141.5, 130.5 (d, $^3J_{CF} = 8.3$ Hz, 1C), 128.0, 126.8 (2C), 125.9 (2C), 123.4 (d, $^4J_{CF} = 2.6$ Hz, 1C), 119.9, 114.1 (d, $^2J_{CF} = 21.5$ Hz, 1C), 113.8 (d, $^2J_{CF} = 20.9$ Hz, 1C), 62.5, not detected at 25 °C: NCH_2 , NCH_3 ; HRMS (ASAP+, m/z): found 364.1574, calcd for $C_{20}H_{19}N_5OF$ $[M+H]^+$ 364.1574.

5.11. N-methyl-N-(4-fluorobenzyl)-8-(4-(hydroxymethyl)phenyl)-9H-purin-6-amine (6g)

The compound was synthesized according to General Procedure 3 using **17g** (26.4 mg, 0.059 mmol). The oil-bath temperature was set to 65 °C and the reaction time was 4 h. Purification by silica-gel flash column chromatography (DCM/MeOH - 9:1, $R_f = 0.35$) gave 19.3 mg (0.053 mmol, 90%) of a colourless powder. 1H NMR (600 MHz, DMSO- d_6) δ 13.50 (s, 1H), 8.24 (s, 1H), 8.09–8.05 (m, 2H), 7.47–7.42 (m, 2H), 7.40–7.35 (m, 2H), 7.19–7.12 (m, 2H), 5.48 (br s, 2H), 5.29 (t, $J = 5.7$ Hz, 1H), 4.55 (d, $J = 5.6$ Hz, 2H), 3.38 (br s, 3H); ^{13}C NMR (151 MHz, DMSO- d_6) δ 161.4 (d, $^1J_{CF} = 242.7$ Hz, 1C), 153.5, 152.9, 151.9, 147.3, 144.5, 134.5, 129.5 (d, $^3J_{CF} = 8.0$ Hz, 2C), 127.9, 126.8 (2C), 125.9 (2C), 119.9, 115.3 (d, $^2J_{CF} = 21.2$ Hz, 2C), 62.5, not detected at 25 °C: NCH_2 , NCH_3 ; HRMS (ASAP+, m/z): found 364.1573, calcd for $C_{20}H_{19}N_5OF$ $[M+H]^+$ 364.1574.

5.12. *N*-(2-Methoxybenzyl)-*N*-methyl-8-(4-(hydroxymethyl)phenyl)-9H-purin-6-amine (6h)

The compound was synthesized according to General Procedure 3 using **17h** (40.6 mg, 0.088 mmol). The reaction time was 2.75 h. Purification by silica-gel flash column chromatography (DCM/MeOH (sat. w/NH₃ – 12.5:1, R_f = 0.23) gave 30.7 mg (0.082 mmol, 93%) of a colourless solid, mp. 250–255 °C; ¹H NMR (600 MHz, DMSO-*d*₆) δ 13.43 (s, 1H), 8.20 (s, 1H), 8.05 (br s, 2H), 7.48–7.39 (m, 2H), 7.25–7.20 (m, 1H), 7.07–7.01 (m, 2H), 6.87–6.82 (m, 1H), 5.28 (br s, 1H), 4.55 (s, 2H), 3.84 (s, 3H), not detected at 25 °C: NCH₂, NCH₃; ¹³C NMR (151 MHz, DMSO-*d*₆) δ 157.1, 153.8, 152.7, 151.8, 147.0, 144.5, 128.0, 128.0, 126.9, 126.7 (2C), 125.9 (2C), 120.3, 120.0, 110.8, 62.5, 55.4, not detected at 25 °C: NCH₂, NCH₃; IR (neat, cm⁻¹): 3400 (br w), 3100 (w), 3070 (w), 2953 (w), 2833 (w), 2722 (w), 1596 (s), 1584 (s), 1489 (m), 1435 (m), 1405 (m), 1333 (m), 1240 (s), 1032 (m), 948 (m), 748 (s); HRMS (ASAP+, *m/z*): found 376.1773, calcd for C₂₁H₂₂N₅O₂ [M+H]⁺ 376.1773.

5.13. *N*-(3-Methoxybenzyl)-*N*-methyl-8-(4-(hydroxymethyl)phenyl)-9H-purin-6-amine (6i)

The compound was synthesized according to General Procedure 3 using **17i** (37.5 mg, 0.082 mmol). The reaction time was 2.5 h. Purification by silica-gel flash column chromatography (DCM/MeOH – 14:1, R_f = 0.21) gave 28.8 mg (0.077 mmol, 94%) of a colourless solid, mp. 258–261 °C; ¹H NMR (400 MHz, DMSO-*d*₆) δ 13.46 (br s, 1H), 8.23 (s, 1H), 8.09–8.07 (m, 2H), 7.45–7.43 (m, 2H), 7.26–7.22 (m, 1H), 6.92–6.85 (m, 2H), 6.85–6.80 (m, 1H), 5.39 (br s, 2H), 5.29 (t, *J* = 5.6 Hz, 1H), 4.55 (d, *J* = 5.4 Hz, 2H), 3.69 (s, 3H), 3.41 (br s, 3H); ¹³C NMR (101 MHz, DMSO-*d*₆) δ 159.4, 153.6, 152.9, 151.9, 147.2, 144.6, 140.0, 129.6, 127.9, 126.8 (2C), 126.0 (2C), 119.9, 119.6, 113.4, 112.2, 62.5, 54.9, not detected at 25 °C: NCH₂, NCH₃; IR (neat, cm⁻¹): 3403 (br w), 3096 (w), 2948 (w), 2921 (w), 2837 (w), 2700 (w), 1596 (s), 1584 (s), 1428 (m), 1403 (m), 1331 (m), 1255 (s), 1158 (m), 1086 (m), 1038 (m), 947 (m), 909 (m), 848 (m), 833 (m), 776 (s); HRMS (ASAP+, *m/z*): found 376.1767, calcd for C₂₁H₂₂N₅O₂ [M+H]⁺ 376.1773.

5.14. *N*-(4-Methoxybenzyl)-*N*-methyl-8-(4-(hydroxymethyl)phenyl)-9H-purin-6-amine (6j)

The compound was synthesized according to General Procedure 3 using **17j** (42.6 mg, 0.093 mmol). The reaction time was 2.5 h. Purification by silica-gel flash column chromatography (DCM/2 M NH₃ in MeOH – 19:1, R_f = 0.19) gave 31.7 mg (0.084 mmol, 91%) of a colourless solid, mp. 265–270 °C. ¹H NMR (600 MHz, DMSO-*d*₆) δ 13.43 (s, 1H), 8.23 (s, 1H), 8.10–8.06 (m, 2H), 7.47–7.42 (m, 2H), 7.29–7.24 (m, 2H), 6.91–6.86 (m, 2H), 5.46 (br s, 2H), 5.28 (t, *J* = 5.7 Hz, 1H), 4.55 (d, *J* = 5.6 Hz, 2H), 3.71 (s, 3H), 3.28 (br s, 3H); ¹³C NMR (151 MHz, DMSO-*d*₆) δ 158.4, 153.5, 152.8, 151.9, 147.1, 144.5, 130.1, 128.9 (2C), 128.0, 126.8 (2C), 125.9 (2C), 119.9, 113.9 (2C), 62.5, 55.0, not detected at 25 °C: NCH₂, NCH₃; (HMBC), See spectrum at 75 °C in the Supporting Information File. IR (neat, cm⁻¹): 3271 (brr w), 2954 (w), 2924 (w), 2832 (w), 2697 (w), 1593 (s), 1513 (s), 1441 (m), 1326 (m), 1303 (m), 1247 (s), 1034 (m), 950 (m), 840 (m), 814 (m), 789 (m), 725 (m), 679 (m); HRMS (ASAP+, *m/z*): found 376.1766, calcd for C₂₁H₂₂N₅O₂ [M+H]⁺ 376.1773.

5.15. *N*-(3,4-Dimethoxybenzyl)-*N*-methyl-8-(4-(hydroxymethyl)phenyl)-9H-purin-6-amine (6k)

The compound was synthesized according to General Procedure 3 using **17k** (34.7 mg, 0.071 mmol). The reaction time was 4 h. Purification by silica-gel flash column chromatography (DCM/MeOH (sat. w/NH₃ – 12.5:1, R_f = 0.22) gave 26.1 mg (0.082 mmol, 91%) of a colourless solid, mp. 254–256 °C; ¹H NMR (600 MHz, DMSO-*d*₆) δ 13.47 (s,

1H), 8.23 (s, 1H), 8.11–8.07 (m, 2H), 7.47–7.43 (m, 2H), 7.03 (s, 1H), 6.90–6.87 (m, 1H), 6.86–6.83 (m, 1H), 5.29 (t, *J* = 5.7 Hz, 1H), 4.55 (d, *J* = 5.3 Hz, 2H), 3.71 (s, 3H), 3.66 (s, 3H), not detected at 25 °C: NCH₂, NCH₃; ¹³C NMR (151 MHz, DMSO-*d*₆) δ 153.5, 152.9, 151.8, 148.7, 148.0, 147.1, 144.5, 130.6, 128.0, 126.8 (2C), 125.9 (2C), 119.9, 119.8, 111.89, 111.85, 62.5, 55.5, 55.4, not detected at 25 °C: NCH₂, NCH₃; IR (neat, cm⁻¹): 3335 (br w), 3101 (w), 3072 (w), 3003 (w), 2954 (w), 2833 (w), 2696 (w), 1586 (s), 1516 (s), 1439 (m), 1403 (m), 1291 (m), 1275 (s), 1259 (s), 1238 (m), 1157 (m), 1028 (s), 837 (m); HRMS (ASAP+, *m/z*): found 406.1875, calcd for C₂₂H₂₄N₅O₃ [M+H]⁺ 406.1879.

5.16. *N*-methyl-*N*-(pyridin-2-ylmethyl)-8-(4-(hydroxymethyl)phenyl)-9H-purin-6-amine (6l)

The compound was synthesized according to General Procedure 3 using **17l** (38 mg, 0.087 mmol). The oil-bath temperature was set to 65 °C and the reaction time was 4 h. Purification by silica-gel flash column chromatography (DCM/MeOH - 9:1, R_f = 0.26) gave 24 mg (0.068 mmol, 78%) of a colourless powder, mp. 284–290 °C (decomp.). ¹H NMR (400 MHz, DMSO-*d*₆) δ 13.24 (s, 1H), 8.57–8.47 (m, 1H), 8.22 (s, 1H), 8.13–7.99 (m, 2H), 7.77–7.69 (m, 1H), 7.49–7.40 (m, 2H), 7.32–7.22 (m, 2H), 5.29 (t, *J* = 5.7 Hz, 1H), 4.55 (d, *J* = 5.6 Hz, 2H), not detected at 25 °C: NCH₃, NCH₂; ¹³C NMR (151 MHz, DMSO-*d*₆) δ 158.0, 153.8, 152.8, 151.8, 149.2, 147.2, 144.5, 136.8, 127.9, 126.8 (2C), 125.9 (2C), 122.2, 121.3, 120.0, 62.5, not detected at 25 °C: NCH₃, NCH₂; HRMS (ASAP+, *m/z*): found 347.1623, calcd for C₁₉H₁₉N₆O [M+H]⁺ 347.1620.

5.17. *N*-methyl-*N*-(pyridin-3-ylmethyl)-8-(4-(hydroxymethyl)phenyl)-9H-purin-6-amine (6m)

The compound was synthesized according to General Procedure 3 using **17m** (22 mg, 0.050 mmol). The oil-bath temperature was set to 65 °C and the reaction time was 4 h. Purification by silica-gel flash column chromatography (DCM/MeOH - 19:1 → 12:1, R_f = 0.20) gave 15 mg (0.042 mmol, 84%) of a colourless powder, mp. 268–270 °C (decomp.). ¹H NMR (600 MHz, DMSO-*d*₆) δ 13.52 (s, 1H), 8.61–8.58 (m, 1H), 8.49–8.45 (m, 1H), 8.25 (s, 1H), 8.10–8.06 (m, 2H), 7.75–7.70 (m, 1H), 7.47–7.42 (m, 2H), 7.37–7.32 (m, 1H), 5.44 (br s, 2H), 5.29 (t, *J* = 5.7 Hz, 1H), 4.55 (d, *J* = 5.6 Hz, 2H), 3.42 (br s, 3H); ¹³C NMR (151 MHz, DMSO-*d*₆) δ 153.5, 153.0, 151.8, 149.0, 148.4, 147.4, 144.6, 135.3, 133.9, 127.9, 126.8 (2C), 126.0 (2C), 123.7, 119.9, 62.5, not detected at 25 °C: NCH₃, NCH₂; HRMS (ASAP+, *m/z*): found 347.1615, calcd for C₁₉H₁₉N₆O [M+H]⁺ 347.1620.

5.18. *N*-methyl-*N*-(pyridin-3-ylmethyl)-8-(4-(hydroxymethyl)phenyl)-9H-purin-6-amine (6n)

The compound was synthesized according to General Procedure 3 using **17n** (25 mg, 0.058 mmol). The oil-bath temperature was set to 65 °C and the reaction time was 7.5 h. Purification by silica-gel flash column chromatography (DCM/MeOH - 19:1, R_f = 0.28) gave 18 mg (0.053 mmol, 91%) of a colourless powder. ¹H NMR (600 MHz, DMSO-*d*₆) δ 13.51 (s, 1H), 8.52–8.48 (m, 2H), 8.24 (s, 1H), 8.08–8.03 (m, 2H), 7.46–7.42 (m, 2H), 7.30–7.26 (m, 2H), 5.46 (br s, 2H), 5.29 (t, *J* = 5.7 Hz, 1H), 4.55 (d, *J* = 5.7 Hz, 2H), 3.47 (br s, 3H); ¹³C NMR (151 MHz, DMSO-*d*₆) δ 153.6, 152.9, 151.8, 149.7 (2C), 147.5, 147.4, 144.6, 127.9, 126.7 (2C), 126.0 (2C), 122.3 (2C), 119.9, 62.5, not detected at 25 °C: NCH₃, NCH₂; HRMS (ASAP+, *m/z*): found 347.1616, calcd for C₁₉H₁₉N₆O [M+H]⁺ 347.1620.

5.19. *N*-methyl-*N*-(2-hydroxybenzyl)-8-(4-(hydroxymethyl)phenyl)-9H-purin-6-amine (6o)

The compound was synthesized according to General Procedure 3

using **17o** (72 mg, 0.162 mmol). The reaction time was 3.5 h. Purification by silica-gel flash column chromatography (DCM/MeOH - 92:8, $R_f = 0.26$) gave 54 mg (0.148 mmol, 92%) of a colourless powder. ^1H NMR (600 MHz, DMSO- d_6) δ 13.47 (s, 1H), 9.94 (s, 1H), 8.22 (s, 1H), 8.10–8.05 (m, 2H), 7.47–7.42 (m, 2H), 7.11–7.05 (m, 2H), 6.86–6.82 (m, 1H), 6.75–6.69 (m, 1H), 5.28 (t, $J = 5.7$ Hz, 1H), 5.03 (br s, 2H), 4.56 (d, $J = 5.6$ Hz, 2H), 3.64 (br s, 3H); ^{13}C NMR (151 MHz, DMSO- d_6) δ 155.5, 153.6, 152.8, 151.7, 147.2, 144.5, 128.4, 128.1, 127.9, 126.7 (2C), 125.9 (2C), 123.8, 119.9, 119.0, 115.4, 62.5, 48.1, not detected at 25 °C: NCH_3 ; HRMS (ASAP+, m/z): found 363.1613, calcd for $\text{C}_{20}\text{H}_{20}\text{N}_5\text{O}_2$ $[\text{M}+\text{H}]^+$ 362.1617.

5.20. *N*-methyl-*N*-(3-trifluoromethylbenzyl)-8-(4-(hydroxymethyl)phenyl)-9H-purin-6-amine (6p)

The compound was synthesized according to General Procedure 3 using **17p** (41 mg, 0.083 mmol). The reaction time was 3.5 h. Purification by silica-gel flash column chromatography (DCM/MeOH - 92.5 : 7.5, $R_f = 0.20$) gave 25 mg (0.060 mmol, 72%) of a colourless powder, mp. 260–262.5 °C. ^1H NMR (600 MHz, DMSO- d_6) δ 13.52 (s, 1H), 8.25 (s, 1H), 8.13–8.00 (m, 2H), 7.81–7.69 (m, 1H), 7.65–7.60 (m, 2H), 7.59–7.55 (m, 1H), 7.46–7.42 (m, 2H), 5.47 (br s, 2H), 5.29 (t, $J = 5.7$ Hz, 1H), 4.55 (d, $J = 5.5$ Hz, 2H), 3.47 (br s, 3H); ^{13}C NMR (151 MHz, DMSO- d_6) δ 153.5, 152.9, 151.9, 147.4, 144.6, 140.0, 131.4, 129.7, 129.2 (q, $^2J_{\text{CF}} = 31.5$ Hz, 1C), 127.9, 126.7 (2C), 125.9 (2C), 124.2 (q, $^1J_{\text{CF}} = 272.1$ Hz, 1C), 124.1 (q, $^3J_{\text{CF}} = 3.1$ Hz, 1C), 123.8 (q, $^3J_{\text{CF}} = 3.8$ Hz, 1C), 119.9, 62.5, 52.4, 36.0; HRMS (ASAP+, m/z): found 414.1543, calcd for $\text{C}_{21}\text{H}_{19}\text{N}_5\text{OF}_3$ $[\text{M}+\text{H}]^+$ 414.1542.

5.21. *N*-methyl-*N*-(thiophen-2-ylmethyl)-8-(4-(hydroxymethyl)phenyl)-9H-purin-6-amine (6q)

The compound was synthesized according to General Procedure 3 using **17q** (50 mg, 0.116 mmol). The reaction time was 1.5 h. Purification by silica-gel flash column chromatography (DCM/MeOH - 20:1 \rightarrow 9:1, $R_f = 0.32$) gave 35 mg (0.099 mmol, 86%) of a colourless powder, mp. 286–293 °C (decomp.). ^1H NMR (600 MHz, DMSO- d_6) δ 13.50 (s, 1H), 8.26 (s, 1H), 8.16–8.05 (m, 2H), 7.52–7.43 (m, 2H), 7.43–7.35 (m, 1H), 7.19–7.11 (m, 1H), 7.01–6.94 (m, 1H), 5.64 (br s, 2H), 4.56 (s, 2H), 3.43 (br s, 3H); ^{13}C NMR (151 MHz, DMSO- d_6) δ 153.0, 152.9, 151.8, 147.4, 144.6, 140.3, 128.0, 126.9, 126.8 (2C), 126.6, 126.0 (2C), 125.9, 120.0, 62.5, 47.8, 35.3; HRMS (ASAP+, m/z): found 352.1236, calcd for $\text{C}_{18}\text{H}_{18}\text{N}_5\text{OS}$ $[\text{M}+\text{H}]^+$ 352.1232.

5.22. *N*-methyl-*N*-(cyclopentylmethyl)-8-(4-(hydroxymethyl)phenyl)-9H-purin-6-amine (6r)

The compound was synthesized according to General Procedure 3 using **17r** (64 mg, 0.151 mmol). The reaction time was 4.0 h. Purification by silica-gel flash column chromatography (DCM/MeOH - 94:6, $R_f = 0.16$) gave 46 mg (0.137 mmol, 91%) of a colourless powder. ^1H NMR (600 MHz, DMSO- d_6) δ 13.39 (s, 1H), 8.18 (s, 1H), 8.10–8.06 (m, 2H), 7.48–7.43 (m, 2H), 5.30 (t, $J = 5.7$ Hz, 1H), 4.56 (d, $J = 5.6$ Hz, 2H), 2.44–2.38 (m, 1H), 1.71–1.61 (m, 4H), 1.52–1.44 (m, 2H), 1.35–1.28 (m, 2H), not detected at 25 °C: NCH_3 , NCH_2 ; ^{13}C NMR (151 MHz, DMSO- d_6) δ 153.7, 152.6, 151.8, 146.7, 144.4, 128.1, 126.8 (2C), 125.8 (2C), 119.8, 62.5, 38.7; (HSQC), 29.7 (2C), 24.6 (2C), not detected at 25 °C: NCH_3 , NCH_2 ; HRMS (ASAP+, m/z): found 338.1980, calcd for $\text{C}_{19}\text{H}_{24}\text{N}_5\text{O}$ $[\text{M}+\text{H}]^+$ 338.1981.

5.23. *N*-methyl-*N*-(cyclohexylmethyl)-8-(4-(hydroxymethyl)phenyl)-9H-purin-6-amine (6s)

The compound was synthesized according to General Procedure 3 using **17s** (40 mg, 0.092 mmol). The oil-bath temperature was set to 65 °C and the reaction time was 6 h. Purification by silica-gel flash

column chromatography (DCM/MeOH - 14:1, $R_f = 0.18$) gave 27 mg (0.078 mmol, 85%) of a colourless powder, mp. 289–296 °C (decomp.). ^1H NMR (600 MHz, DMSO- d_6) δ 13.36 (s, 1H), 8.18 (s, 1H), 8.13–8.03 (m, 2H), 7.52–7.38 (m, 2H), 5.29 (t, $J = 5.6$ Hz, 1H), 4.56 (d, $J = 5.5$ Hz, 2H), 1.97–1.82 (m, 1H), 1.73–1.63 (m, 4H), 1.63–1.55 (m, 1H), 1.27–1.09 (m, 3H), 1.09–0.97 (m, 2H), not detected at 25 °C: NCH_3 , NCH_2 ; ^{13}C NMR (151 MHz, DMSO- d_6) δ 153.8, 152.6, 151.8, 146.7, 144.4, 128.2, 126.8 (2C), 125.8 (2C), 119.8, 62.5, 36.6, 30.1 (2C), 26.1, 25.4 (2C), not detected at 25 °C: NCH_3 , NCH_2 ; HRMS (ASAP+, m/z): found 352.2139, calcd for $\text{C}_{20}\text{H}_{26}\text{N}_5\text{O}$ $[\text{M}+\text{H}]^+$ 352.2137.

5.24. *N*-methyl-*N*-(tetrahydrofuran-2-ylmethyl)-8-(4-(hydroxymethyl)phenyl)-9H-purin-6-amine (6t)

The compound was synthesized according to General Procedure 3 using **17t** (54 mg, 0.128 mmol). The oil-bath temperature was set to 70 °C and the reaction time was 2.5 h. Purification by silica-gel flash column chromatography (DCM/MeOH - 92.5 : 7.5, $R_f = 0.15$) gave 40 mg (0.118 mmol, 92%) of a colourless powder. ^1H NMR (600 MHz, DMSO- d_6) δ 13.39 (s, 1H), 8.19 (s, 1H), 8.10–8.06 (m, 2H), 7.48–7.44 (m, 2H), 5.29 (t, $J = 5.7$ Hz, 1H), 4.56 (d, $J = 5.6$ Hz, 2H), 4.24–4.19 (m, 1H), 3.81–3.75 (m, 1H), 3.65–3.58 (m, 1H), 2.01–1.94 (m, 1H), 1.94–1.87 (m, 1H), 1.84–1.74 (m, 1H), 1.65–1.58 (m, 1H), not detected at 25 °C: NCH_3 , NCH_2 ; ^{13}C NMR (151 MHz, DMSO- d_6) δ 153.6, 152.6, 151.8, 146.9, 144.4, 128.1, 126.8 (2C), 125.8 (2C), 120.0, 77.6, 67.1, 62.5, 54.0, 36.4, 28.6, 25.0; HRMS (ASAP+, m/z): found 340.1774, calcd for $\text{C}_{18}\text{H}_{22}\text{N}_5\text{O}_2$ $[\text{M}+\text{H}]^+$ 340.1773.

5.25. *N*-methyl-*N*-(tetrahydrofuran-3-ylmethyl)-8-(4-(hydroxymethyl)phenyl)-9H-purin-6-amine (6u)

The compound was synthesized according to General Procedure 3 using **17u** (51 mg, 0.120 mmol). The oil-bath temperature was set to 70 °C and the reaction time was 2.5 h. Purification by silica-gel flash column chromatography (DCM/MeOH - 92.5 : 7.5, $R_f = 0.15$) gave 35 mg (0.103 mmol, 86%) of a colourless powder. ^1H NMR (600 MHz, DMSO- d_6) δ 13.42 (s, 1H), 8.20 (s, 1H), 8.11–8.07 (m, 2H), 7.48–7.44 (m, 2H), 5.30 (t, $J = 5.8$ Hz, 1H), 4.56 (d, $J = 4.7$ Hz, 2H), 3.85–3.79 (m, 1H), 3.79–3.74 (m, 1H), 3.67–3.61 (m, 1H), 3.53–3.48 (m, 1H), 2.75 (app hept, $J = 7.1$ Hz, 1H), 2.00–1.91 (m, 1H), 1.71–1.62 (m, 1H), not detected at 25 °C: NCH_3 , NCH_2 ; ^{13}C NMR (151 MHz, DMSO- d_6) δ 153.6, 152.7, 151.8, 147.0, 144.4, 128.1, 126.8 (2C), 125.8 (2C), 119.9, 70.4, 66.9, 62.5, 51.9, 38.2, 36.3, 29.5; HRMS (ASAP+, m/z): found 340.1778, calcd for $\text{C}_{18}\text{H}_{22}\text{N}_5\text{O}_2$ $[\text{M}+\text{H}]^+$ 340.1773.

5.26. *N*-methyl-*N*-(oxan-2-ylmethyl)-8-(4-(hydroxymethyl)phenyl)-9H-purin-6-amine (6v)

The compound was synthesized according to General Procedure 3 using **17v** (55 mg, 0.125 mmol). The reaction time was 1.5 h. Purification by silica-gel flash column chromatography (DCM/MeOH - 9:1, $R_f = 0.28$) gave 34 mg (0.096 mmol, 77%) of a colourless powder. ^1H NMR (600 MHz, DMSO- d_6) δ 13.18 (s, 1H), 8.19 (s, 1H), 8.09–8.05 (m, 2H), 7.48–7.44 (m, 2H), 5.29 (t, $J = 5.7$ Hz, 1H), 4.56 (d, $J = 5.3$ Hz, 2H), 3.90–3.84 (m, 1H), 3.72–3.65 (m, 1H), 3.33–3.25 (m, 1H), 1.81–1.74 (m, 1H), 1.71–1.68 (m, 1H), 1.50–1.38 (m, 3H), 1.30–1.24 (m, 1H); ^{13}C NMR (151 MHz, DMSO- d_6) δ 153.6, 152.6, 151.8, 146.9, 144.4, 128.1, 126.8 (2C), 125.8 (2C), 119.9, 77.5, 67.4, 62.5, 55.3, 37.3, 28.7, 25.6, 22.7; HRMS (ASAP+, m/z): found 354.1931, calcd for $\text{C}_{19}\text{H}_{24}\text{N}_5\text{O}_2$ $[\text{M}+\text{H}]^+$ 354.1930.

5.27. *N*-methyl-*N*-(oxan-4-ylmethyl)-8-(4-(hydroxymethyl)phenyl)-9H-purin-6-amine (6w)

The compound was synthesized according to General Procedure 3 using **17w** (54 mg, 0.123 mmol). The reaction time was 4 h. Purification

by silica-gel flash column chromatography (DCM/MeOH - 19:1 → 12:1, $R_f = 0.17$) gave 39 mg (0.109 mmol, 88%) of a colourless powder. ^1H NMR (600 MHz, DMSO- d_6) δ 13.35 (s, 1H), 8.19 (s, 1H), 8.12–8.05 (m, 2H), 7.49–7.41 (m, 2H), 5.29 (t, $J = 5.7$ Hz, 1H), 4.56 (d, $J = 5.6$ Hz, 2H), 3.86–3.80 (m, 2H), 3.29–3.22 (m, 2H), 2.17–2.06 (m, 1H), 1.61–1.51 (m, 2H), 1.40–1.27 (m, 2H), not detected at 25 °C: NCH_3 , NCH_2 ; ^{13}C NMR (151 MHz, DMSO- d_6) δ 153.8, 152.6, 151.8, 146.8, 144.4, 128.1, 126.8 (2C), 125.8 (2C), 119.8, 66.7 (2C), 62.5, 55.3, 36.5, 34.1, 30.2 (2C); HRMS (ASAP+, m/z): found 354.1930, calcd for $\text{C}_{19}\text{H}_{24}\text{N}_5\text{O}_2$ $[\text{M}+\text{H}]^+$ 354.1930.

5.28. *N*-methyl-*N*-(1-methylpiperidin-3-ylmethyl)-8-(4-(hydroxymethyl)phenyl)-9H-purin-6-amine (6x)

The compound was synthesized according to General Procedure 3 using **17x** (43 mg, 0.095 mmol) and $\text{HCl}_{(\text{aq})}$ (0.1 mL, 37%). The reaction time was 1.5 h. Purification by silica-gel flash column chromatography (DCM/MeOH (sat. w/ NH_3) - 92.5 : 7.5, $R_f = 0.11$) gave 32 mg (0.087 mmol, 91%) of a colourless powder, mp. >249 °C (decomp.). ^1H NMR (600 MHz, DMSO- d_6) δ 13.38 (s, 1H), 8.19 (s, 1H), 8.11–8.06 (m, 2H), 7.48–7.44 (m, 2H), 5.29 (s, 1H), 4.56 (s, 2H), 2.69–2.66 (m, 1H), 2.63–2.57 (m, 1H), 2.15–2.10 (m, 1H), 2.11 (s, 3H), 1.86–1.83 (m, 1H), 1.78–1.75 (m, 1H), 1.68–1.59 (m, 2H), 1.46–1.39 (m, 1H), 1.04–0.99 (m, 1H), not detected at 25 °C: NCH_2 , NCH_3 ; ^{13}C NMR (151 MHz, DMSO- d_6) δ 153.7, 152.6, 151.8, 146.8, 144.4, 128.1, 126.8 (2C), 125.8 (2C), 119.8, 62.5, 59.4, 55.8, 53.7, 46.5, 36.9, 35.6, 27.4, 24.4; HRMS (ASAP+, m/z): found 367.2251, calcd for $\text{C}_{20}\text{H}_{27}\text{N}_6\text{O}$ $[\text{M}+\text{H}]^+$ 367.2251.

5.29. *N*-methyl-*N*-(1-benzylpiperidin-4-ylmethyl)-8-(4-(hydroxymethyl)phenyl)-9H-purin-6-amine (6y)

The compound was synthesized according to General Procedure 3 using **17y** (51 mg, 0.097 mmol) and $\text{HCl}_{(\text{aq})}$ (0.1 mL, 37%). The reaction time was 1 h. Purification by silica-gel flash column chromatography (DCM/MeOH (sat. w/ NH_3) - 92.5 : 7.5, $R_f = 0.21$) gave 38 mg (0.087 mmol, 89%) of a pale yellow powder. ^1H NMR (600 MHz, DMSO- d_6) δ 13.38 (s, 1H), 8.18 (s, 1H), 8.11–8.07 (m, 2H), 7.48–7.44 (m, 2H), 7.31–7.23 (m, 4H), 7.23–7.19 (m, 1H), 5.29 (t, $J = 5.7$ Hz, 1H), 4.56 (d, $J = 5.5$ Hz, 2H), 3.40 (s, 2H), 2.81–2.75 (m, 2H), 1.92–1.82 (m, 3H), 1.64–1.58 (m, 2H), 1.36–1.27 (m, 2H), not detected at 25 °C: NCH_2 , NCH_3 ; ^{13}C NMR (151 MHz, DMSO- d_6) δ 153.7, 152.6, 151.8, 146.7, 144.4, 138.7, 128.6 (2C), 128.11, 128.06 (2C), 126.8 (2C), 126.7, 125.8 (2C), 119.8, 62.5, 62.4, 52.9 (2C), 29.5 (2C); HRMS (ASAP+, m/z): found 443.2556, calcd for $\text{C}_{26}\text{H}_{31}\text{N}_6\text{O}$ $[\text{M}+\text{H}]^+$ 443.2559.

5.30. *N*-Benzyl-8-phenyl-9H-purin-6-amine (7)

The compound was synthesized according to General Procedure 2 using the bromide **13** (50 mg, 0.163 mmol), phenylboronic acid (24 mg, 0.194 mmol), Pd-PEPPSI-SIPr (5.5 mg, 0.0081 mmol) and K_2CO_3 (68 mg, 0.495 mmol) in 1,4-dioxane (1.0 mL) and water (1.0 mL). The reaction was stirred on an oil-bath (100 °C) for 2 h. Purification by trituration (H_2O) and recrystallization from 1,4-dioxane (~0.1 mL/mg), filtering and washing with Et_2O gave 8 mg (0.027 mmol, 17%) of a colourless solid. ^1H NMR (600 MHz, DMSO- d_6) δ 13.44 (s, 1H), 8.28 (s, 1H), 8.19 (s, 1H), 8.17–8.13 (m, 2H), 7.56–7.51 (m, 2H), 7.51–7.46 (m, 1H), 7.40–7.36 (m, 2H), 7.33–7.27 (m, 2H), 7.27–7.18 (m, 1H), 4.72 (s, 2H); ^{13}C NMR (151 MHz, DMSO- d_6) δ 153.9, 152.5, 151.2, 148.1, 140.3, 129.81, 129.78, 128.9 (2C), 128.2 (2C), 127.2 (2C), 126.6, 126.1 (2C), 120.0, 42.9; HRMS (ES+, m/z): found 302.1409, calcd for $\text{C}_{18}\text{H}_{16}\text{N}_5$ $[\text{M}+\text{H}]^+$ 302.1406.

5.31. 4-(6-(Benzylamino)-9H-purin-8-yl)phenylmethanol (8)

The compound was synthesized according to General Procedure 2

using the bromide **13** (50 mg, 0.165 mmol), 4-(hydroxymethyl)phenylboronic acid (30 mg, 0.199 mmol), XPhos (4.2 mg, 0.0088 mmol), XPhos Pd G2 (6.4 mg, 0.0081 mmol) and K_2CO_3 (68 mg, 0.494 mmol) in 1,4-dioxane (1.0 mL) and water (1.0 mL). The reaction was stirred on an oil-bath (100 °C) for 2 h 20 min. Purification by trituration (H_2O) and recrystallization from isopropanol/1,4-dioxane (~0.1 mL/mg) gave 25 mg (0.075 mmol, 45%) of a colourless solid. ^1H NMR (600 MHz, DMSO- d_6) δ 13.38 (s, 1H), 8.26 (s, 1H), 8.18 (s, 1H), 8.12–8.08 (m, 2H), 7.49–7.45 (m, 2H), 7.40–7.36 (m, 2H), 7.33–7.27 (m, 2H), 7.24–7.18 (m, 1H), 5.30 (t, $J = 5.7$ Hz, 1H), 4.73 (s, 2H), 4.57 (d, $J = 5.3$ Hz, 2H), 3.56 (s, 1H); ^{13}C NMR (151 MHz, DMSO- d_6) δ 153.8, 152.4, 151.1, 148.2, 144.5, 140.3, 128.2 (2C), 128.0, 127.3 (2C), 126.8 (2C), 126.6, 126.0 (2C), 119.9, 62.5, 42.9; HRMS (ES+, m/z): found 332.1515, calcd for $\text{C}_{19}\text{H}_{18}\text{N}_5\text{O}$ $[\text{M}+\text{H}]^+$ 332.1511.

5.32. *N*-methyl-*N*-(oxan-4-ylmethyl)-8-(4-(2-hydroxyethyl)phenyl)-9H-purin-6-amine (9)

Compound **16w** (68 mg, 0.149 mmol) was treated as described in General Procedure 2 using 4-(2-hydroxyethyl)phenylboronic acid (31 mg, 0.184 mmol), $\text{PdCl}_2(\text{dppf})$ (5.3 mg, 0.0072 mmol) and K_2CO_3 (62 mg, 0.446 mmol) in 1,4-dioxane (1.4 mL) and water (0.7 mL). The reaction was stirred on an oil-bath (80 °C) for 10 min. Purification by silica-gel flash column chromatography (EtOAc, $R_f = 0.14$) gave 64 mg (0.142 mmol, 95%) of a colourless solid, mp. 65–135 °C. ^1H NMR (400 MHz, CDCl_3) δ 8.37 (s, 1H), 7.82–7.75 (m, 2H), 7.42–7.35 (m, 2H), 5.59 (dd, $J = 11.2, 2.2$ Hz, 1H), 4.29–4.21 (m, 1H), 4.03 (br s, 2H), 4.01–3.91 (m, 4H), 3.75–3.64 (m, 1H), 3.45 (br s, 3H), 3.41–3.30 (m, 2H), 3.08–2.93 (m, 3H), 2.19–2.07 (m, 1H), 2.03–1.96 (m, 1H), 1.88–1.73 (m, 1H), 1.68–1.34 (m, 7H); ^{13}C NMR (101 MHz, CDCl_3) δ 154.7, 152.2, 152.0, 148.9, 140.6, 129.9, 129.3, 129.1, 120.0, 83.9, 68.9, 67.8, 63.4, 39.1, 34.6 (HSQC), 30.5, 28.5, 24.8, 23.5, not detected at 25 °C: CH_2NCH_3 ; HRMS (ASAP+, m/z): found 452.2659, calcd for $\text{C}_{25}\text{H}_{34}\text{N}_5\text{O}_3$ $[\text{M}+\text{H}]^+$ 452.2662.

The THP protected intermediate from above (56 mg, 0.123 mmol) was treated as described in General Procedure 3 using $\text{HCl}_{(\text{aq})}$ (0.1 mL, 37%). The reaction time was 2 h 20 min. Purification by silica-gel flash column chromatography (DCM/MeOH - 14:1, $R_f = 0.14$) gave 40 mg (0.109 mmol, 88%) of a colourless powder, mp. 261.5–264.5 °C (decomp.). ^1H NMR (600 MHz, DMSO- d_6) δ 13.37 (s, 1H), 8.19 (s, 1H), 8.05–8.01 (m, 2H), 7.39–7.35 (m, 2H), 4.68 (t, $J = 5.2$ Hz, 1H), 3.86–3.80 (m, 2H), 3.64 (td, $J = 6.9, 4.5$ Hz, 2H), 3.28–3.21 (m, 2H), 2.78 (t, $J = 6.9$ Hz, 2H), 2.16–2.06 (m, 1H), 1.58–1.52 (m, 2H), 1.38–1.28 (m, 2H), not detected at 25 °C: NCH_2 , NCH_3 ; ^{13}C NMR (151 MHz, DMSO- d_6) δ 153.7, 152.6, 151.7, 146.9, 141.6, 129.5 (2C), 127.4, 125.8 (2C), 119.8, 66.7 (2C), 61.9, 55.3, 38.8, 36.2, 34.2, 30.2 (2C); HRMS (ESI+, m/z): found 368.2086, calcd for $\text{C}_{20}\text{H}_{26}\text{N}_5\text{O}_2$ $[\text{M}+\text{H}]^+$ 368.2087.

6. Biochemical assays

6.1. CSF1R enzymatic inhibitory assay

The compounds were supplied in a 10 mM DMSO solution, and enzymatic CSF1R inhibition potency was determined by Invitrogen (ThermoFisher) using their Z'-LYTE® assay technology [37]. The assay is based on fluorescence resonance energy transfer (FRET). In the primary reaction, the kinase transfers the gamma-phosphate of ATP to a single tyrosine residue in a synthetic FRET-peptide. In the secondary reaction, a site-specific protease recognizes and cleaves non-phosphorylated FRET-peptides. Thus, phosphorylation of FRET-peptides suppresses cleavage by the development reagent. Cleavage disrupts FRET between the donor (i.e. coumarin) and acceptor (i.e., fluorescein) fluorophores on the FRET-peptide, whereas uncleaved, phosphorylated FRET-peptides maintain FRET. A ratiometric method, which calculates the ratio (the emission ratio) of donor emission to

acceptor emission after excitation of the donor fluorophore at 400 nm, is used to quantitate inhibition. All compounds were first tested for their inhibitory activity at 500 nM in duplicates. The potency observed at 500 nM was used to set starting point of the IC₅₀ titration curve, in which two levels were used 1000 or 10000 nM. The IC₅₀ values reported are based on the average of at least 2 titration curves (minimum 20 data points), and were calculated from activity data with a four parameter logistic model using SigmaPlot (Windows Version 12.0 from Systat Software, Inc.) Unless stated otherwise the ATP concentration used was equal to K_M (ca 10 mM).

6.2. Kinase binding assay (Kd)

Kinase-tagged T7 phage strains were prepared in an *E. coli* host derived from the BL21 strain. *E. coli* were grown to log-phase and infected with T7 phage and incubated with shaking at 32 °C until lysis. The lysates were centrifuged and filtered to remove cell debris. The remaining kinases were produced in HEK-293 cells and subsequently tagged with DNA for qPCR detection. Streptavidin-coated magnetic beads were treated with biotinylated small molecule ligands for 30 min at room temperature to generate affinity resins for kinase assays. The ligand beads were blocked with excess biotin and washed with blocking buffer (SeaBlock (Pierce), 1% BSA, 0.05% Tween 20, 1 mM DTT) to remove unbound ligand and to reduce non-specific binding. Binding reactions were assembled by combining kinases, liganded affinity beads, and test compounds in 1x binding buffer (20% SeaBlock, 0.17x PBS, 0.05% Tween 20, 6 mM DTT). Test compounds were prepared as 111X stocks in 100% DMSO. Kds were determined using an 11-point 3-fold compound dilution series with three DMSO control points. All compounds for Kd measurements are distributed by acoustic transfer (non-contact dispensing) in 100% DMSO. The compounds were then diluted directly into the assays such that the final concentration of DMSO was 0.9%. All reactions performed in polypropylene 384-well plate. Each was a final volume of 0.02 mL. The assay plates were incubated at room temperature with shaking for 1 h and the affinity beads were washed with wash buffer (1x PBS, 0.05% Tween 20). The beads were then re-suspended in elution buffer (1x PBS, 0.05% Tween 20, 0.5 μM non-biotinylated affinity ligand) and incubated at room temperature with shaking for 30 min. The kinase concentration in the eluates was measured by qPCR. Binding constants (Kds) were calculated with a standard dose-response curve using the Hill equation with the Hill Slope was set to -1. Curves were fitted using a non-linear least squares fit with the Levenberg-Marquardt algorithm. The experiments were performed by Eurofins.

6.3. Kinase panel

The kinase panel assays was run as described above, but at a single concentration (500 nM). The experiments were performed by Eurofins.

6.4. Effect of CSF1R inhibitors on p-ERK1/2 in mouse bone-marrow derived macrophages

Bone-marrow derived macrophages were obtained by flushing the femur and tibia of sacrificed mice with HBSS (Hanks' balanced salt solution) using a syringe with a 25G needle. The cells were centrifuged at 1500 rpm for 8 min, the resulting supernatant was decanted, and the cells resuspended in 5 mL RBC (red blood cell) lysis buffer. Lysis was stopped by adding 30 mL medium containing 10% FCS (Fetal Calf Serum). The cells were centrifuged at 1500 rpm for 8 min. The supernatant was decanted, and the cells resuspended in RPMI medium gentamycin, 2 mM glutamine, 10% FCS) with 10 ng/mL CSF-1 (colony stimulating factor 1). The cells were seeded in bacteria plates. After two days, fresh medium with 10 ng/mL CSF-1 was added and after another two days, 50% of the medium was replaced with fresh medium containing 10 ng/mL CSF-1 while the other 50% is centrifuged to get rid of

dead cells before being transferred back to the cells. After incubating for one week, the differentiated cells were washed twice with PBS, added PBS EDTA (0.2 mM) and incubated for 10 min. Cells were detached by scraping and centrifuged at 1200 rpm for 7 min. The supernatant was decanted, and the cells resuspended in RPMI medium (10% FCS, 10 ng/mL CSF-1, x gentamycin, 2 mM L-glutamine). The cells were seeded out in 96-well glass bottom plates (Cellvis) at 50,000 cells in 100 μL per well and incubated at 37 °C overnight. The medium was removed, and the cells washed three times with PBS before being starved overnight in 0.1% FCS medium without CSF-1. CSF1R inhibitors dissolved in DMSO, was added to the wells in appropriate concentrations and incubated for 30 min at 37 °C. DMSO was added to control wells at the highest inhibitor concentration. CSF-1 (0.1 mg/mL) was added to all wells except the CSF-1 negative control to obtain an end concentration of CSF-1 of 10 ng/mL. After incubating for another 10 min at 37 °C, the cells were fixed by adding PFA (paraformaldehyde) (16%) to obtain an end concentration of 4% for 10 min. The cells were washed twice with TBS, and permeabilized by MeOH for 10 min on ice. The cells were washed twice with TBS and blocked in Odyssey blocking solution (Licor, #927-60001) diluted 1:1 in TBS-Tween (0,1%) for 1.5 h under careful agitation. The blocking solution was removed and the wells added appropriately diluted primary antibody solution (P-MAPK (ERK1/2, Thr202/Tyr204) (CST, #4370, rabbit) 1:1200 and MAPK (ERK1/2), (Biolegend, #686902, rat) 1:300 in Odyssey blocking buffer:TBS-Tween (1:1)). After incubating overnight with careful shaking at 4 °C, the cells were washed with TBST 5 times for 5 min while agitating. Secondary antibody solution was added, and the wells were incubated for 1 h in the dark R dye 800CW goat anti-rabbit and IR dye 680RD goat anti-rat diluted 1:800 in Odyssey blocking buffer:TBS-Tween (1:1). The antibody solution was removed, and the wells were washed 4 × 5 min with TBST and 2 × 5 min with TBS while carefully agitating. The TBS was removed, and the plate was scanned on a Licor Odyssey scanner. Using Image Studio software, the intensity of fluorescence of each well is recorded after subtracting the background noise (wells not added primary antibody). The results were normalized by dividing the P-MAPK intensity with total MAPK intensity for all the wells. The average value of triplicate wells was calculated for every concentration of inhibitor used. The average values are then divided by the CSF-1 positive control value. PLX3397 was included as a reference on all plates. Due to some inter-assay variation the activity of the inhibitors is also reported as fold change relative to PLX3397 (Fold change: IC₅₀ inhibitor/IC₅₀ PLX3397).

6.5. Osteoclast differentiation assay

Human Osteoclast Precursor Cells (Lonza, # 2T-110) were seeded, directly upon thawing, in 96-well uClear plates (Greiner) at 1 × 10⁴ cells per well in MEM α (Gibco, # 41061029) media containing 10% FBS, 2 mM L-Glutamine, 1% P/S. Cells were differentiated with 66 ng/mL RANKL and 33 ng/mL M-CSF in presence of varying concentrations of compounds (1 μM–10 pM, 10-fold dilutions). OPG (33 ng/mL), osteoprotegerin, was used as positive control for osteoclastogenesis inhibition. Cells were differentiated over 7 days, and growth media with supplements/compounds was renewed every 3 days. Following treatment cells were fixed with 3.2% PFA (Electron Microscopy Sciences), permeabilized with 0.1% TritonX-100 (Sigma), and stained with 50 μg/mL TRITC-Phalloidin (Sigma) and 1 μg/mL Hoechst (Thermo Fisher Scientific) in 1% BSA for 40 min at RT. Images were acquired using ImageXpress Micro high-content imaging system (Molecular Devices) with 1 field/well using 4 × objective and capturing DAPI (Hoechst) and TxRed (TRITC-Phalloidin). Image analysis was performed manually using the ImageJ-cell counter plugin (osteoclast identified as large cells with ≥3 nuclei) or using a custom developed analysis module in MetaXpress (Molecular Devices). First, the pipeline identified Nuclei from the DAPI, based on size and signal threshold. The Nuclei mask was then expanded by 5 pixels, to create 'Undifferentiated Cell Mask'. Phalloidin positive signal from TxRed channel, was extracted using simple

thresholding based only on signal intensity, to create 'Total Cell Mask'. Finally, the two masks were subtracted to provide 'Differentiated Cell Mask'. Degree of osteoclast differentiation was measured by calculating Phalloidin stained area using the 'Differentiated Cell Mask' and normalizing it to the nuclei count. We considered Osteoclast count in RANKL/M-CSF only treated cells as maximum differentiation (Max Ctrl, 100%), while OPG treatment in presence of RANKL/M-CSF as undifferentiated cells (Min Ctrl, 0%). The percentage effect for each compound was calculated as follows: %effect = $100 \times [1 - (\text{test compound} - \text{average min control}) / (\text{average Max control} - \text{average min control})]$. The IC₅₀ values were calculated using four parameters logistic model (4 PL) in XLfit (Fit model 205). Each condition was tested in triplicates.

6.6. In vivo pharmacokinetic study

The in vivo pharmacokinetic profiling of **6w**, **9** and PLX3397 was evaluated in female C57BLKS mice (n = 3) by cassette intravenous (iv) single dosing of drugs (1 mg/kg each) in a 20% DMSO, 80% PEG400 formulation. Blood sampling was done after 10, 30, 60, 120, 240 and 480 min. The work, following the EU Directive 2010/63/EU for animal experiments, was conducted under the global project 2017072717008661#10796 V8 approved by the ethical committee and national authorities (CEEA-LR-n°036 – authorization number 10796) on November 27th, 2019 for 5 years and was conducted at Eurofins ADME Bioanalyses, 30310 Vergèze, France (accreditation number D303441). Analysis was performed by LCMS.

6.7. Molecular modelling

Molecular modelling was carried out using the Maestro software package on the Schrödinger Platform (Maestro, v12.4.079, release 2020.2; Schrödinger, LLC, New York, USA). An x-ray structure of CSF1R with PDB-ID 6T2W was prepared using the protein preparation wizard. Bond orders and formal charges were added for het-groups and hydrogens were added to all atoms in the system. Water molecules beyond 5 Å from het-groups were removed. An all-atom constrained minimization was performed using the OPLS3 force field. Ligands drawn in ChemBioDraw Ultra (v19.1, CambridgeSoft, PerkinElmer) were prepared using LigPrep (Schrödinger) and subsequently docked in the binding site of the energy minimized protein construct receptor grid of 6T2W as defined by the co-crystallized ligand using GLIDE in SP mode [38].

Declaration of competing interest

The authors declare the following financial interests/personal relationships which may be considered as potential competing interests: Several of the authors contributing to the work is employed at Lead Discovery Center GmbH (LDC) a translational drug discovery organization. Some of the reported work in this manuscript is part of patent application number 2215113.8.

Data availability

Data will be made available on request.

Acknowledgements

The support from the Research Council of Norway to the project (Grant number: NFR 284937) and the Norwegian NMR Platform (project number 226244/F50) are highly appreciated. So is the help from the Mass Spectrometry Lab at the NV Faculty at NTNU. Roger Aarvik is thanked for technical support. Elisabeth Hjøllø and Jori Kveberg Skinderhaug are acknowledged for initial synthetic work. Prof. Unni Syversen (Department of Clinical and Molecular Medicine, NTNU) is thanked for her contribution to assay development.

Appendix A. Supplementary data

Supplementary data to this article can be found online at <https://doi.org/10.1016/j.ejmech.2023.115344>. This file contains synthesis and characterization of intermediates, NMR spectra, description of ADME assays, enzymatic inhibition titration curves and additional references [39–44].

References

- [1] V. Chitu, C.I. Caescu, R. S. J. Lennartsson, L. Rönstrand, C.H. Heldin, The PDGFR Receptor family, in: *Receptor Tyrosine Kinases: Family and Subfamilies*, Springer International Publishing, Switzerland, 2015.
- [2] A. Kumari, O. Silakari, R.K. Singh, Recent advances in colony stimulating factor-1 receptor/c-FMS as an emerging target for various therapeutic implications, *Biomed. Pharmacother.* 103 (2018) 662–679, <https://doi.org/10.1016/j.biopha.2018.04.046>.
- [3] M.A. Cannarile, M. Weisser, W. Jacob, A.-M. Jegg, C.H. Ries, D. Rüttinger, Colony-stimulating factor 1 receptor (CSF1R) inhibitors in cancer therapy, *J. Immunother. Cancer* 5 (2017) 53, <https://doi.org/10.1186/s40425-017-0257-y>.
- [4] M.I. El-Gamal, S.K. Al-Ameen, D.M. Al-Koumi, M.G. Hamad, N.A. Jalal, C.H. Oh, Recent advances of colony-stimulating factor-1 receptor (CSF-1R) kinase and its inhibitors, *J. Med. Chem.* 61 (2018) 5450–5466, <https://doi.org/10.1021/acs.jmedchem.7b00873>.
- [5] B.F. Boyce, E. Rosenberg, A.E. de Papp, L.T. Duong, The osteoclast, bone remodelling and treatment of metabolic bone disease, *Eur. J. Clin. Invest.* 42 (2012) 1332–1341, <https://doi.org/10.1111/j.1365-2362.2012.02717.x>.
- [6] S.H. Mun, P.S.U. Park, K.-H. Park-Min, The M-CSF receptor in osteoclasts and beyond, *Exp. Mol. Med.* 52 (2020) 1239–1254, <https://doi.org/10.1038/s12276-020-0484-z>.
- [7] J.G. Conway, B. McDonald, J. Parham, B. Keith, D.W. Rusnak, E. Shaw, M. Jansen, P. Lin, A. Payne, R.M. Crosby, J.H. Johnson, L. Frick, M.-H.J. Lin, S. Depee, S. Tadeipalli, B. Votta, I. James, K. Fuller, T.J. Chambers, F.C. Kull, S. D. Chamberlain, J.T. Hutchins, Inhibition of colony-stimulating-factor-1 signaling in vivo with the orally bioavailable cFMS kinase inhibitor GW2580, *Proc. Natl. Acad. Sci. U. S. A.* 102 (2005) 16078–16083, <https://doi.org/10.1073/pnas.0502000102>.
- [8] C. Zhang, P.N. Ibrahim, J. Zhang, E.A. Burton, G. Habets, Y. Zhang, B. Powell, B. L. West, B. Matusow, G. Tsang, R. Shellooe, H. Carias, H. Nguyen, A. Marimuthu, K. Y. Zhang, A. Oh, R. Bremer, C.R. Hurt, D.R. Artis, G. Wu, M. Nespi, W. Spevak, P. Lin, K. Nolop, P. Hirth, G.H. Tesch, G. Bollag, Design and pharmacology of a highly specific dual FMS and KIT kinase inhibitor, *Proc. Natl. Acad. Sci. U. S. A.* 110 (2013) 5689–5694, <https://doi.org/10.1073/pnas.1219457110>.
- [9] X.-F. Wang, Y.-j. Wang, T.-y. Li, J.-x. Guo, F. Lv, C.-l. Li, X.-t. Ge, Colony-stimulating factor 1 receptor inhibition prevents against lipopolysaccharide-induced osteoporosis by inhibiting osteoclast formation, *Biomed. Pharmacother.* 115 (2019), 108916, <https://doi.org/10.1016/j.biopha.2019.108916>.
- [10] G. Hedger, M.S.P. Sansom, H. Koldso, The juxtamembrane regions of human receptor tyrosine kinases exhibit conserved interaction sites with anionic lipids, *Sci. Rep.* 5 (2015) 9198, <https://doi.org/10.1038/srep09198>.
- [11] S.R. Hubbard, Juxtamembrane autoinhibition in receptor tyrosine kinases, *Nat. Rev. Mol. Cell Biol.* 5 (2004) 464–471, <https://doi.org/10.1038/nrm1399>.
- [12] L.M. Wodicka, P. Ciceri, M.I. Davis, J.P. Hunt, M. Floyd, S. Salerno, X.H. Hua, J. M. Ford, R.C. Armstrong, P.P. Zarrinkar, D.K. Treiber, Activation state-dependent binding of small molecule kinase inhibitors: structural insights from biochemistry, *Chem. Biol.* 17 (2010) 1241–1249, <https://doi.org/10.1016/j.chembiol.2010.09.010>.
- [13] C. Schubert, C. Schalk-Hihi, G.T. Struble, H.C. Ma, I.P. Petrounia, B. Brandt, I. C. Deckman, R.J. Patch, M.R. Player, J.C. Spurlino, B.A. Springer, Crystal structure of the tyrosine kinase domain of colony-stimulating factor-1 receptor (cFMS) in complex with two inhibitors, *J. Biol. Chem.* 282 (2007) 4094–4101, <https://doi.org/10.1074/jbc.M608183200>.
- [14] S.M. Hanson, G. Georgiou, M.K. Thakur, W.T. Miller, J.S. Rest, J.D. Chodera, M. A. Seeliger, What makes a kinase promiscuous for inhibitors? *Cell Chem. Biol.* 26 (2019) 390–399, <https://doi.org/10.1016/j.chembiol.2018.11.005>.
- [15] S. Eathiraj, R. Palma, M. Hirschi, E. Volkova, E. Nakuci, J. Castro, C.R. Chen, T. C. Chan, D.S. France, M.A. Ashwell, A novel mode of protein kinase inhibition exploiting hydrophobic motifs of autoinhibited kinases: discovery of ATP-independent inhibitors of fibroblast growth factor receptor, *J. Biol. Chem.* 286 (2011) 20677–20687, <https://doi.org/10.1074/jbc.M110.213736>.
- [16] K. Ikegashira, T. Ikenogami, T. Yamasaki, T. Oka, Y. Hase, N. Miyagawa, K. Inagaki, I. Kawahara, Y. Koga, H. Hashimoto, Optimization of an azetidone series as inhibitors of colony stimulating factor-1 receptor (CSF-1R) Type II to lead to the clinical candidate JTE-952, *Bioorg. Med. Chem. Lett.* 29 (2019) 873–877, <https://doi.org/10.1016/j.bmcl.2019.02.006>.
- [17] S.A. Ramachandran, P.S. Jadhavar, S.K. Miglani, M.P. Singh, D.P. Kalane, A. K. Agarwal, B.D. Sathe, K. Mukherjee, A. Gupta, S. Haldar, M. Raja, S. Singh, S. M. Pham, S. Chakravarty, K. Quinn, S. Belmar, I.E. Alfaro, C. Higgs, S. Bernales, F. J. Herrera, R. Rai, Design, synthesis and optimization of bis-amide derivatives as CSF1R inhibitors, *Bioorg. Med. Chem. Lett.* 27 (2017) 2153–2160, <https://doi.org/10.1016/j.bmcl.2017.03.064>.
- [18] G. Burnstock, Purine and purinergic receptors, *Brain Neurosci. Adv.* 2 (2018), 2398212818817494, <https://doi.org/10.1177/2398212818817494>.

- [19] Z. Tang, W. Ye, H. Chen, X. Kuang, J. Guo, M. Xiang, C. Peng, X. Chen, H. Liu, Role of purines in regulation of metabolic reprogramming, *Purinergic Signal*. 15 (2019) 423–438, <https://doi.org/10.1007/s11302-019-09676-z>.
- [20] H. Rosemeyer, The chemodiversity of purine as a constituent of natural products, *Chem. Biodivers.* 1 (2004) 361–401, <https://doi.org/10.1002/cbdv.200490033>.
- [21] S. Sharma, J. Singh, R. Ojha, H. Singh, M. Kaur, P.M.S. Bedi, K. Nepali, Design strategies, structure activity relationship and mechanistic insights for purines as kinase inhibitors, *Eur. J. Med. Chem.* 112 (2016) 298–346, <https://doi.org/10.1016/j.ejmech.2016.02.018>.
- [22] A.M. Gilbert, P. Nowak, N. Brooijmans, M.G. Bursavich, C. Dehnhardt, E.D. Santos, L.R. Feldberg, I. Hollander, S. Kim, S. Lombardi, K. Park, A.M. Venkatesan, R. Mallon, Novel purine and pyrazolo[3,4-d]pyrimidine inhibitors of PI3 kinase I α : hit to lead studies, *Bioorg. Med. Chem. Lett* 20 (2010) 636–639, <https://doi.org/10.1016/j.bmcl.2009.11.051>.
- [23] W.-S. Huang, X. Zhu, Y. Wang, M. Azam, D. Wen, R. Sundaramoorthi, R. M. Thomas, S. Liu, G. Banda, S.P. Lentini, S. Das, Q. Xu, J. Keats, F. Wang, S. Wardwell, Y. Ning, J.T. Snodgrass, M.I. Broudy, K. Russian, G.Q. Daley, J. Iulicci, D.C. Dalgarno, T. Clackson, T.K. Sawyer, W.C. Shakespeare, 9-(Arenethenyl)purines as dual Src/Abl kinase inhibitors targeting the inactive conformation: design, synthesis, and biological evaluation, *J. Med. Chem.* 52 (2009) 4743–4756, <https://doi.org/10.1021/jm900166t>.
- [24] N. Ibrahim, L. Mouawad, M. Legraverend, Novel 8-arylated purines as inhibitors of glycogen synthase kinase, *Eur. J. Med. Chem.* 45 (2010) 3389–3393, <https://doi.org/10.1016/j.ejmech.2010.04.026>.
- [25] S.J. Kaspersen, J. Han, K.G. Nørsett, L. Rydså, E. Kjøbli, S. Bugge, G. Bjørkøy, E. Sundby, B.H. Hoff, Identification of new 4-N-substituted 6-aryl-7H-pyrrolo[2,3-d]pyrimidine-4-amines as highly potent EGFR-TK inhibitors with Src-family activity, *Eur. J. Pharmaceut. Sci.* 59 (2014) 69–82, <https://doi.org/10.1016/j.ejps.2014.04.011>.
- [26] C.S. Leung, S.S.F. Leung, J. Tirado-Rives, W.L. Jorgensen, Methyl effects on protein–ligand binding, *J. Med. Chem.* 55 (2012) 4489–4500, <https://doi.org/10.1021/jm3003697>.
- [27] J. Michel, J. Tirado-Rives, W.L. Jorgensen, Energetics of displacing water molecules from protein binding sites: consequences for ligand optimization, *J. Am. Chem. Soc.* 131 (2009) 15403–15411, <https://doi.org/10.1021/ja906058w>.
- [28] T.K. Darling, T.J. Lamb, Emerging roles for Eph receptors and Ephrin ligands in immunity, *Front. Immunol.* 10 (2019), <https://doi.org/10.3389/fimmu.2019.01473>.
- [29] Y. Dong, J. Pan, Y. Ni, X. Huang, X. Chen, J. Wang, High expression of EphB6 protein in tongue squamous cell carcinoma is associated with a poor outcome, *Int. J. Clin. Exp. Pathol.* 8 (2015) 11428–11433, <https://pubmed.ncbi.nlm.nih.gov/26617870/>.
- [30] A. El Zawily, E. McEwen, B. Toosi, F.S. Vizeacoumar, T. Freywald, F. J. Vizeacoumar, A. Freywald, The EphB6 receptor is overexpressed in pediatric T cell acute lymphoblastic leukemia and increases its sensitivity to doxorubicin treatment, *Sci. Rep.* 7 (2017) 1–10, <https://doi.org/10.1038/s41598-017-15200-3>.
- [31] B.M. Toosi, A. El Zawily, L. Truitt, M. Shannon, O. Allonby, M. Babu, J. DeCoteau, D. Mousseau, M. Ali, T. Freywald, A. Gall, F.S. Vizeacoumar, M.W. Kirzinger, C. R. Geyer, D.H. Anderson, T. Kim, A.L. Welm, P. Siegel, F.J. Vizeacoumar, A. Kusalik, A. Freywald, EPHB6 augments both development and drug sensitivity of triple-negative breast cancer tumours, *Oncogene* 37 (2018) 4073–4093, <https://doi.org/10.1038/s41388-018-0228-x>.
- [32] C. Abad-Zapatero, Ligand efficiency indices for effective drug discovery, *Expert Opin. Drug Discov.* 2 (2007) 469–488, <https://doi.org/10.1517/17460441.2.4.469>.
- [33] P. Saharinen, M. Vihinen, O. Silvennoinen, Autoinhibition of Jak2 tyrosine kinase is dependent on specific regions in its pseudokinase domain, *Mol. Biol. Cell* 14 (2003) 1448–1459, <https://doi.org/10.1091/mbc.e02-06-0342>.
- [34] C.R.W. Guimarães, B.K. Rai, M.J. Munchhof, S. Liu, J. Wang, S.K. Bhattacharya, L. Buckbinder, Understanding the impact of the P-loop conformation on kinase selectivity, *J. Chem. Inf. Model.* 51 (2011) 1199–1204, <https://doi.org/10.1021/ci200153c>.
- [35] N. Ibrahim, F. Chevot, M. Legraverend, Regioselective Sonogashira cross-coupling reactions of 6-chloro-2,8-diiodo-9-THP-9H-purine with alkyne derivatives, *Tetrahedron Lett.* 52 (2011) 305–307, <https://doi.org/10.1016/j.tetlet.2010.11.033>.
- [36] M.C. Wenlock, R.P. Austin, P. Barton, A.M. Davis, P.D. Leeson, A comparison of physicochemical property profiles of development and marketed oral drugs, *J. Med. Chem.* 46 (2003) 1250–1256, <https://doi.org/10.1021/jm021053p>.
- [37] B.A. Pollok, B.D. Hamman, S.M. Rodems, L.R. Makings, *Optical Probes and Assays*, 2000. WO 2000066766 A1.
- [38] T.A. Halgren, R.B. Murphy, R.A. Friesner, H.S. Beard, L.L. Frye, W.T. Pollard, J. L. Banks, Glide: a new approach for rapid, accurate docking and scoring. 2. Enrichment factors in database screening, *J. Med. Chem.* 47 (2004) 1750–1759, <https://doi.org/10.1021/jm030644s>.